

# Effect of urban morphology on microclimate and building cluster energy consumption in cold regions of China



Peng Cui<sup>a</sup>, Jiaqi Lu<sup>a,\*</sup>, Yutong Wu<sup>b</sup>, Jingnan Tang<sup>a</sup>, Jinjian Jiang<sup>a</sup>

<sup>a</sup> College of Landscape Architecture, Northeast Forestry University, Harbin 150040, China

<sup>b</sup> College of Architecture and Art Design, Inner Mongolia University of Science and Technology, Inner Mongolia 014010, China

## ARTICLE INFO

### Keywords:

Urban morphology  
Energy consumption  
Microclimate  
Regression analysis  
Severe cold region

## ABSTRACT

Building energy consumption (BEC) is influenced by the combination of urban morphology and microclimate. This study investigated the influence of urban neighborhood morphology on microclimate and building energy consumption through sixty representative street blocks in cold regions of China. The following conclusions were drawn from the multiple regression analysis, and random forest (RF) in this research: 1) The impact of urban morphology on microclimate and vice versa on energy use intensity (EUI) varies according to the season. 2) Annual temperature (TEMP.), solar radiation (SR), building site cover (BSC), average building height (BH), road area ratio (RAR), and block orientation (BO) were significantly positively correlated with EUI, and the floor area ratio (FAR) was negatively correlated. 3) The FAR is positively correlated with BEC and has a significant negative correlation with relative humidity (RH) which contribution rates are 82.3 % and 7.3 %, respectively. Based on the analysis, the research proposed feasible recommendations to optimize the layout of blocks. The results of this study can be used to predict the energy consumption of new and existing street blocks in cold-climate cities quickly and accurately. Additionally, it provides quantitative strategies for energy-saving and emission reduction in urban planning.

## 1. Introduction

Building energy consumption (BEC), due to rapid urbanization, accounts for 40 % of the global annual energy consumption and 36 % of carbon emissions, and it has been on a continuously increasing trend (Bui, Nguyen, Ngo, & Nguyen-Xuan, 2020; Somu, MR, & Ramamritham, 2021; Yang, Chen, Wang, Li, & Li, 2016). Excessive BEC affects the environment by contributing to global warming and air pollution (Dandotiya & Sharma, 2021; Olu-Ajayi, Alaka, Sulaimon, Sunmola, & Ajayi, 2022; Santamouris, 2020). Therefore, reducing BEC is the key to realizing the urban emission reduction and alleviating the urban heat island effect. Especially for cities in cold regions, the energy consumption for heating during winter is high, which hinders their ecological and low-carbon development. Therefore, exploring the influence mechanism of building cluster layout on the change in energy consumption under severely cold climates is urgently required.

Urban morphology is an important factor affecting BEC (Ahn & Sohn, 2019; Xu et al., 2021). Street morphology, building group layout pattern, building site cover, floor area ratio, sky view factor, road coverage, total area of surface wall, and landscape pattern affect the

energy consumption of a neighborhood (Hadavi & Pasdarshahri, 2021; Lu et al., 2023; Quan & Li, 2021; Shan, Deng, Tang, Wu, & Wang, 2022; Sharifi, 2019; Uçlar & Buldurur, 2020; Xi, Ren, Wang, Feng, & Cao, 2021). Among them, FAR is the most critical factor in energy-efficient heating (Leng, Chen, Ma, Wong, & Ming, 2020). Building density affects the natural lighting and passive solar gains of a building, and urban canyons affect energy use in offices by as much as +30 % and up to +19 % in residential areas of Copenhagen (Strømann-Andersen & Sattrup, 2011). The diversity of orientation designs and heights was also observed to lead to a reduction in cooling loads of 6.4 % and 4.6 % between the base case and urban neighborhood configurations, respectively (Shareef, 2021). The height-to-width ratio (H/W) of urban streets has a marked effect on BEC, followed by street orientation. The peak cooling energy consumption of buildings with H/W = 0.5 street valleys is 37.13 % higher than that of buildings with H/W = 2.0 street valleys (Huang & Li, 2017). In addition, research has shown that urban morphology varies widely in the extent to which it affects BEC in different climatic zones, some scholars have long utilized climate as an intermediary factor to investigate its impact on BEC (Javanroodi & Nik, 2019).

\* Corresponding author.

E-mail addresses: [cuipeng@nefu.edu.cn](mailto:cuipeng@nefu.edu.cn) (P. Cui), [lujiaqi@nefu.edu.cn](mailto:lujiaqi@nefu.edu.cn) (J. Lu).

Urban morphology has a direct impact on BEC by influencing the microclimate surrounding the building (Ma, Wang, Wang, & Chen, 2022; Wong et al., 2011). Microclimate factors include temperature (TEMP.), relative humidity (RH), solar radiation (SR), and wind speed (WS). Among these, SR is the most significant factor influencing the energy consumption of building clusters (Wang, Liu, & Zhang, 2021; Yue, Yan, Ni, Lei, & Qin, 2024). It found that ignoring the effect of microclimate on energy consumption in July and January overestimated heat loads by about 20 % and underestimated cooling loads by 30 % in some European cities (Boccalatte, Fossa, Gaillard & Menezo, 2020). Outdoor temperature significantly affects the heat load of the building through convection and conduction heat transfer. Different wind speeds can have a direct impact on convective exchange and air infiltration in buildings, which can affect the energy consumption of buildings (Hadavi & Pasdarshahri, 2020). Previous studies also showed that when the ambient wind speed decreases from 4 m/s to 0.5 m/s, the air temperature can increase by up to 1.3 K (Memon, Leung & Liu, 2010). Yang et al., (2020) evaluated the impact of urban heat islands on building energy performance by measuring hourly air temperature and relative humidity for three consecutive years in 10 neighborhoods in Nanjing, China. The experiments showed that heat islands can increase the cooling demand of residential buildings by 12 % to 24 % and reduce heating demand by 3 % to 20 %. Wong et al., (2011) developed a prediction model to investigate the impact of different air temperatures on BEC. Their results revealed that rational regional planning could lower outdoor temperatures by approximately 1 °C, leading to a reduction in air conditioning energy consumption. Notably, the quantitative research on the relationship between urban morphology, microclimate, and energy consumption is relatively mature. However, fewer studies have considered all three factors together. Regarding the three dynamic coupling research methodologies, the currently popular methodology involves statistical fitting: after obtaining the energy consumption of a city or neighborhood, mathematical correlation equations are established using morphological and microclimate data. Energy consumption data are obtained as electricity consumption or coal consumption for conversion. For instance, the land surface temperature (LST) method uses a one-to-one quadratic regression fit of the electricity consumption data to the simulated energy consumption to derive correlation coefficients for later estimation (Chen, Han & De Vries, 2020). The dynamic analysis of the three elements at the urban scale is based on the surface wind speed and temperature, which are obtained from infrared satellites, and the dynamic coupling equations of the three elements are established by estimating urban energy consumption data and extracting GIS data. However, correcting the microclimate data obtained by this method is challenging, as significant deviations in the calculations often occur. Therefore, accurately quantifying the relationship between the three elements at the neighborhood scale has become a pressing concern in the field of urban energy consumption.

Currently, applications for predicting building energy can be classified into three main types: numerical, analytical, and predictive methods (Ahmad, Mourshed & Rezgui, 2017). With significant advances in the application of computational intelligence (CI) techniques, ensemble-based methods in predictive methods (e.g., RF, etc.) do not require much fine-tuning of their parameters, and often the default parameters yield excellent performance (Ahmad, Mourshed, & Rezgui, 2017; Bourdeau, qiang Zhai, Nefzaoui, Guo, & Chatellier, 2019). TRNSYS, UMI, NetLogo, and decision models such as Random forests, decision trees, ANN and GNN were, currently used for analyzing energy consumption predictions at the neighborhood and city scale (Seyedzadeh, Rahimian, Rastogi & Glesk, 2019). Scholars often combine different methods to analyze and process data to obtain more accurate and effective experimental results. For example, Xie et al. (2023) found that EUI is mainly affected by Average length of the block, Shape factor, and Building density by using Honeybee for simulation and multiple regression model to build the dependent equation. Wang et al. (2022) found that relative compactness, building coverage, and building height

have a significant impact on office building cluster's energy performance by EnergyPlus and enhanced global sensitivity analysis in sub-tropical monsoonal climate.

Research on building energy utilization has become increasingly in-depth. However, there are still some shortcomings in the existing studies. 1) The change in building cluster energy consumption is influenced by urban morphology and climatic background, making it challenging to generalize studies across different geographic regions (Zhao et al., 2024). This challenge is particularly evident in cold climates, where energy consumption is significant, yet there is a lack of related research. 2) At the level of research methodology, the current research at the neighborhood and city scale mostly focuses on theoretical models. Furthermore, scholars often select a single urban morphology factor to analyze the impact of building and cluster energy consumption, or they overlay the energy consumption of individual buildings to derive cluster energy consumption data. There is less emphasis on considering the influence of building cluster patterns on microclimate, which indirectly affects building energy consumption and leads to large errors. 3) The existing studies conclude establishing simulation methods or exploring energy consumption impact mechanisms, rather than applying the findings effectively to low-carbon urban planning practices.

To fill this gap, This study focuses on optimizing the outdoor microclimate and reducing BEC by altering the multi-urban morphology parameters. This research aims to enhance the human environment and mitigate the urban heat island effect. Accordingly, The study selects Harbin, a representative city in the cold region of China. This research selects 60 typical street blocks and calculates the morphology factors of building clusters for four energy-using types by integrating data from various sources. The study then collects microclimate and energy usage data from different layouts through measurements and simulations. The purposes of the study are 1) exploring the effects of morphology layout such as FAR, BSC, BH, Road Height Width Ratio (RHR), RAR, Green Space Ratio (GSR), Total Wall Surface Area (WSA), Sky View Factor (SVF), Block Orientation (BO) and microclimate(TEMP., SR, RH, WS) on energy consumption at the street block scale in cold regions, and develop multiple regression fitting equations for urban morphology, microclimate, and energy consumption. 2) exploring the impact of urban morphology and microclimate influencing factors on BEC in the cold region city using RF for prediction, 3) exploring the relative impact of energy consumption in various types of street blocks and suggesting optimal building layouts for different neighborhood types in the central city of a frigid region to decrease overall building energy usage. Aiming to fill the gap in understanding regional climatic impacts and the integration of energy consumption and microclimate within urban morphology.

## 2. Study area and methods

### 2.1. Research framework

This study was conducted in four stages: data collection and processing, indicator selection and computation, data analysis and evaluation, and impact analysis and recommendation, as shown in Fig. 1. First, vector data were obtained and preprocessed, and the factors that may affect the BEC in the neighborhood were obtained through a literature search and preliminary screening of the data. Subsequently, the impact factors were calculated, and BEC in the sample neighborhood was simulated. Simultaneously, the gathered data were examined and processed to eliminate outliers, and a multiple regression model (MLR) was created using urban morphology factors and the factors affecting microclimate as independent variables and building energy use as dependent variables. Finally, the RF model was used to determine the contribution of the selected factors to the neighborhood-scale BEC.

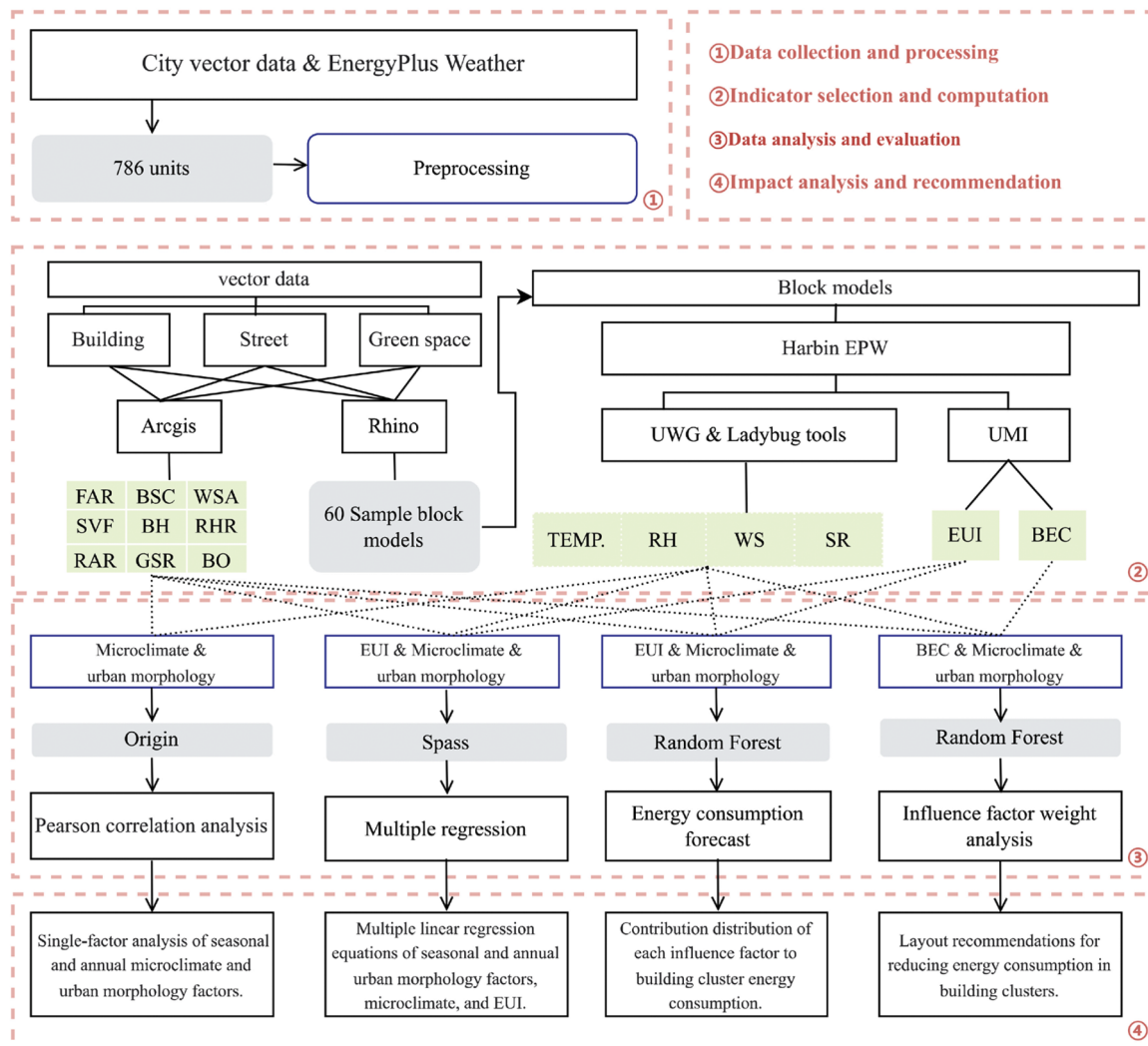


Fig. 1. Research flowchart.

## 2.2. Study area and climatic contexts

Harbin, the capital of Heilongjiang Province, is an important transportation, political, economic, and financial center in Northeast China. According to the *Harbin Statistical Yearbook 2021*, Harbin is divided into nine districts and nine counties, covering an area of 53,076.5 km<sup>2</sup>, with a built-up area of 10,192.8 km<sup>2</sup>. The major urban area is divided into four road loops: the second road loop mostly consists of the old urban area, the third loop primarily consists of the old urban area and the new development zone, and the fourth road loop is the region to be developed. The study area is depicted in Fig. 2(a).

Harbin belongs to the mid-temperate continental monsoon climate, which is characterized by four distinct seasons. It experiences cold winters with an average temperature of -19 °C, hot summers with an average temperature of 23 °C, a snowy period from November to January, and the highest wind speeds in the spring. The lowest wind speeds occur in the winter, with predominantly southwesterly winds (Zhang, Cui & Song, 2020). The climate of the last 10 years is depicted in Fig. 3. Harbin is a typical city in China located in a severely cold region with 180 days of heating. Buildings have cooling demands in summer and heating demands in winter. Therefore, it is essential to study the energy consumption of the city in this area to achieve energy savings in buildings.

## 2.3. Data sources and processing methods

### 2.3.1. Urban morphological data

There is 10–30 % of BEC influenced by urban morphology (Rickwood, Glazebrook, & Searle, 2008; Strømann-Andersen & Sattrup, 2011; Zhang, Yan, Liu, & Qiao, 2021). Block-scale building clusters are the fundamental unit of urban composition. Their layout influences the heat exchange balance inside and outside the buildings, thus directly impacting energy exchange. This, in turn, indirectly alters energy usage behaviors and ultimately affects BEC. Regarding BEC, the influence factor of urban morphology in the severe cold region is not clear. The research is based on quantifying three perspectives: buildings, streets, and greenery. Through literature analysis, the research identifies and organizes the factors influencing urban morphology that significantly impact the energy consumption of building clusters in various geographic regions. After comparison, nine types of representative neighborhood-scale urban morphology influencing factors are identified, as shown in Table 1.

Because the third road loop covers part of the new city and the old city is the city center of Harbin, the neighborhood types are more complete. Therefore, this study selected the area within the third road loop for its scope, as shown in Fig. 2(a). First, the research obtained the basic vector data of buildings, roads, green spaces, etc. in Harbin City by crawling the latest online map (OSM). And analyzing the data by GIS to acquire data related to all 9 types of neighborhood morphology

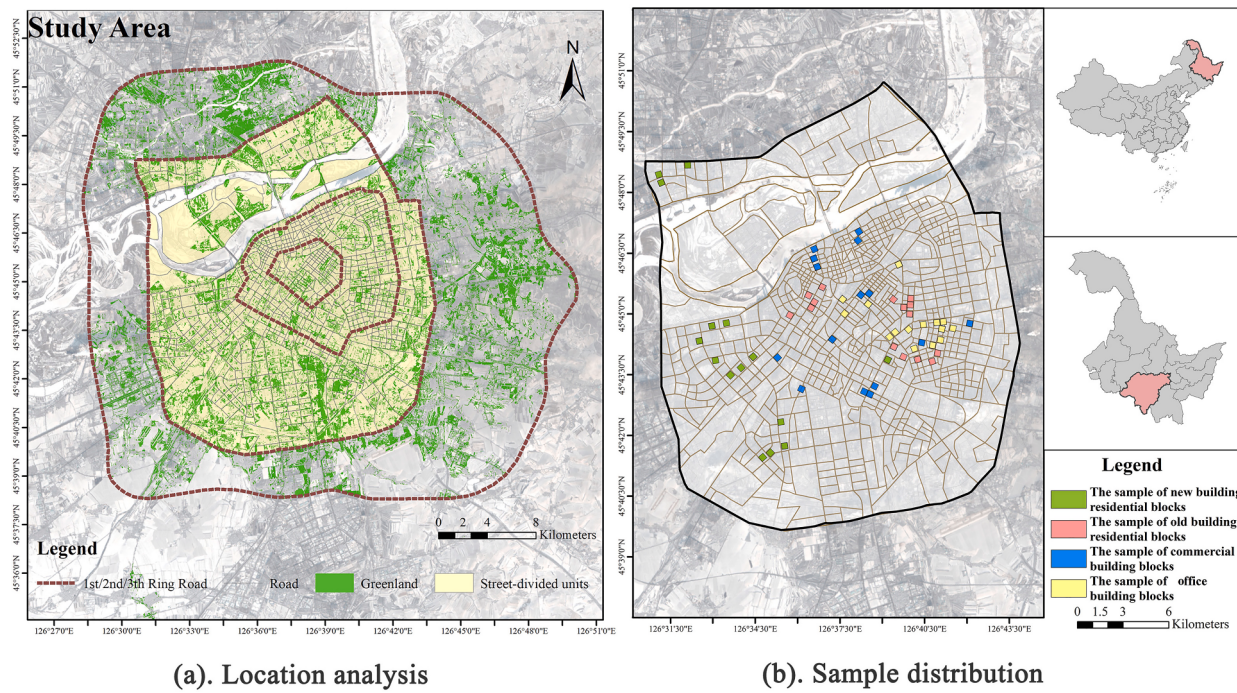


Fig. 2. Study area analysis and sample distribution map.

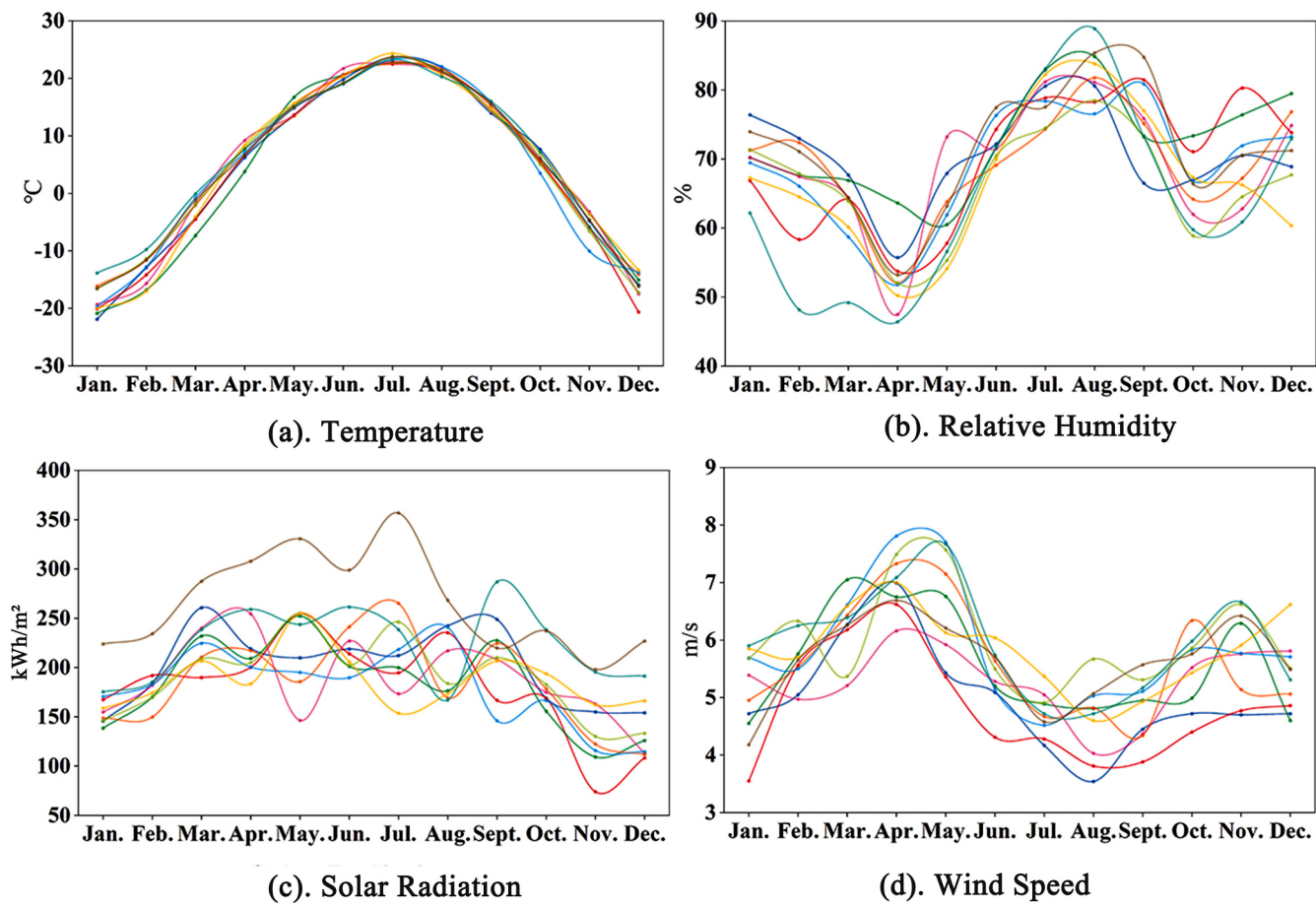


Fig. 3. Average climate data for Harbin by month, 2013–2023.

**Table 1**  
Urban morphology impact factor.

Indicator	Formula	Meaning	Calculation method
Floor Area Ratio (FAR)	$FAR = \sum S_{Floor} / S_{Block}$	The ratio of the total floor area of buildings on a site to the net land area of that site.	ArcGIS calculation tools
Building Site Cover(BSC)	$BSC = \sum S_{Footprint} / S_{Block}$	Refers to the ratio of the total base area of the building to the occupied area within a certain range.	ArcGIS calculation tools
Building Height(BH)	$BH = \sum (S_{Footprint} \times H) / \sum S_{Footprint}$	Average height of the buildings in the sample area.	ArcGIS calculation tools
Road Height width Ratio (RHR)	$RHR = [\sum L_{Road} (H_{Building} / W_{Road})] / \sum L_{Road}$	The ratio of the average building height and street width on either sides of a street.	ArcGIS calculation tools
Road Area Ratio(RAR)	$RAR = \sum S_{Road} / S_{Block}$	The ratio of the road area to the plots.	ArcGIS calculation tools
Total Wall Surface Area (WSA)	$WSA = \sum (S_{Facade} + S_{Roof})$	The sum of the building surface area within the sample area.	ArcGIS calculation tools
Green Space Ratio(GSR)	$GSR = S_{Greenspace} / S_{Block}$	The ratio of the sum of all kinds of green space area within the land scope to the land area (%)	ArcGIS calculation tools
Sky View Factor (SVF)	$SVF = 1 - \sum_{i=1}^n \sin \gamma_i / n$	The density, height, shape and other shielding degree of the building to the surrounding environment	ArcGIS calculation tools
Block Orientation(BO)	/	Angle of main road to north.	ArcGIS calculation tools

influence factors of 786 plots within the third loop. The distribution map of the data visualization is shown in Fig. 4. To ensure that the selected samples meet the statistical requirements, box plots were used to normalize the data and select the samples by observing their dispersion, as shown in Fig. 5. Each indicator is located within the 10th and 90th percentile intervals of the box plot. Simultaneously, the research utilizes satellite maps to identify new development areas as the primary selection range for new building blocks, old city areas for old building blocks, typical commercial areas and commercial building clusters for commercial blocks, and office clusters and office circles for office blocks. Finally, based on the aforementioned selection criteria, the research chooses various types of more comprehensive blocks and representative blocks as the experimental block samples.

The street blocks of Harbin can be divided into three categories: point-cluster, row-type, and courtyard-type neighborhoods. Building clusters within the range of 100–500 m have the most significant degree of influence on the changes in microclimate, and the morphology is easier to control and adjust (Zhang et al., 2020). The block scale in the Harbin area is 300 m × 300 m–600 m × 600 m, so according to the block structure and function type, a 400 × 400 m rectangle was chosen as the study range of the sample block. BEC is influenced by energy usage behavior. To reflect this, 15 typical blocks from each of the four categories—old residential building blocks, new residential building blocks, commercial street building districts, and office building blocks—were chosen as representatives. These blocks cover various neighborhood types in the primary urban area of Harbin City, showcasing a diverse spatial morphology. The distribution of samples is illustrated in Fig. 2 (b), and the morphology of the sample street blocks is detailed in Appendix B.

### 2.3.2. Microclimate data acquisition

To obtain more accurate BEC data, this study used the microclimate simulation computing tool, urban weather generator (UWG), developed by MIT for simulation (Bueno, Norford, Hidalgo & Pigeon, 2013). UWG estimates the urban energy consumption of the urban area through a multi-scale urban climatology model coupled with TMY data of the suburban weather station and the known key morphology of the urban area, such as the FAR and the street aspect ratio. It can also produce output in EPW format to be imported into the dynamic building energy simulation software for simulating the BEC under the influence of the urban heat island (Bueno, Roth, Norford & Li, 2014). An evaluation of the UWG based on yes-drop data from Basel and Toulouse revealed that the prediction error of the UWG stays within the range of temperature variations observed at different locations in the same urban area (Bueno

et al., 2013). Additionally, EPW files can be used for building energy simulation, and for small office buildings and single-family houses, the difference in actual EUI between urban and rural areas is 13 % and 17 %, respectively, which is reduced to 8 % and 13 % by the UWG (Street, Reinhart, Norford & Ochsendorf, 2013). Ladybug tools complement the missing module for calculating sunlight intensity in the UWG (Tehrani, Veisi, Fakhr & Du, 2024).

### 2.3.3. Building energy consumption calculations

The sample was divided into three categories according to the time of construction: 1986–1996, 1997–2007, and 2008–present. Neighborhood functions were divided into four categories: new residential, old residential, commercial, and office buildings, of which commercial buildings and office buildings are public buildings. To better control the variables in the experiment, this research selected building samples with the most similar physical properties. Based on the Chinese energy-saving design standards: *Energy conservation design standard for heating residential buildings*, *Design standard for energy efficiency of residential buildings in Heilongjiang Province*, *Design standard for energy efficiency of residential buildings in severe cold and cold zones*, and *Design standard for energy efficiency of public buildings*, this research selected buildings with similar shape coefficients, window-to-wall ratios, and floor areas as the samples and investigated the thermal characteristics of the maintenance structures in the field, which confirms that these buildings have similar heat transfer coefficients, as listed in Table 2.

The energy consumption in building clusters was studied using UMI, an urban cluster simulation plugin based on the Rhino parametric design platform. The UMI adopts the Shoebox Model, which combines the thermal characteristics (function, orientation, external shading, etc.) of a single unit into a large area. The Shoebox Model clusters and combines similar parts of a single unit into a large area and calculates the energy intensity of the corresponding representative unit modules in the large area, and then sums them according to the weights (Dogan & Reinhart, 2017). The Shoebox Model has good accuracy and reliability. The model requires a small difference in temperature settings between zones and needs to simplify the model while reducing the impact on the simulation accuracy, thus striking a balance between the addition time and the validity of the results. The specific modeling steps of the UMI are shown in Fig. 6.

Firstly, the model was converted to the format applicable to UMI; data modifications and adjustments were then made to the UMI database; subsequently, the EPW weather file was imported, and the building parameters were modified; and finally, the results were exported. After describing the model, Dogan and Reinhart (2017) demonstrated the

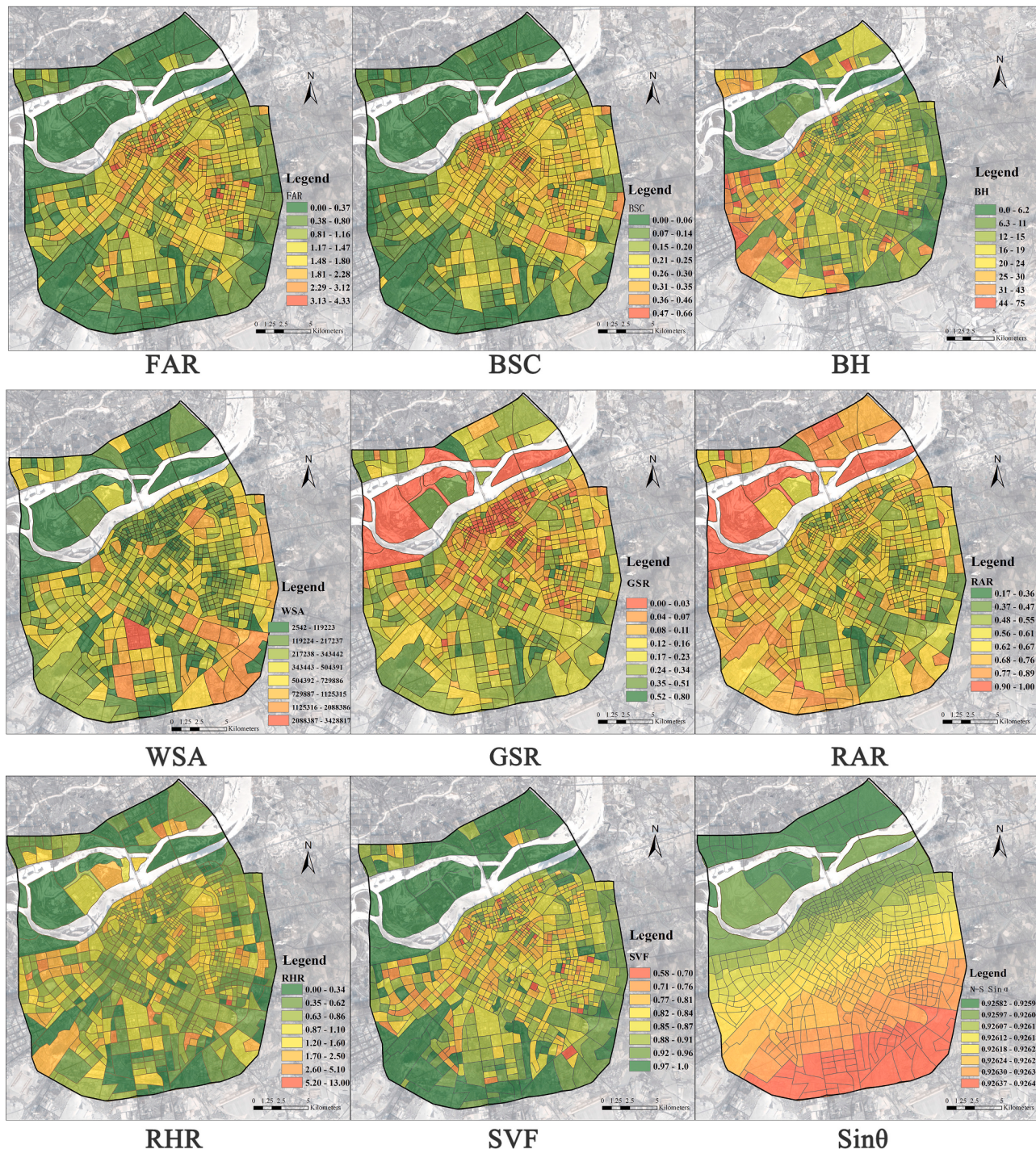


**Fig. 4.** Distribution of factors influencing urban morphology in the study area.(Where N-S sin $\theta$  is the value of the plot prime and (0,0)).

model's ability to generate load profiles for a mixed-use neighborhood consisting of 121 fully regulated buildings under a variety of climatic conditions. To validate energy consumption, 20 % of the 60 sample street blocks with access to electricity data were investigated. The electricity consumption data was obtained from the total neighborhood energy consumption of the governmental electricity department in the study area. After conducting a regression analysis of the energy consumption data with the simulated data, an  $R^2$  value of 0.875 was obtained. The results of UMI's building energy simulation in this study were found to be more accurate and research meaningful through validation.

#### 2.4. Statistical analyses

This study used MLR and RF models to quantify the impact of urban spatial elemental indicators on energy consumption in building clusters, calculate the weights of the influencing factors, and perform predictive analysis. In MLR, the value of the dependent variable is predicted by a linear combination of a set of independent variables. The method aims to build a model that explains the variability of the dependent variable and predicts the change in the dependent variable by making changes to the independent variables. In MLR analysis, the independent variable is usually represented as a vector, whereas the dependent variable is represented as a scalar. The basic form of MLR can be expressed as

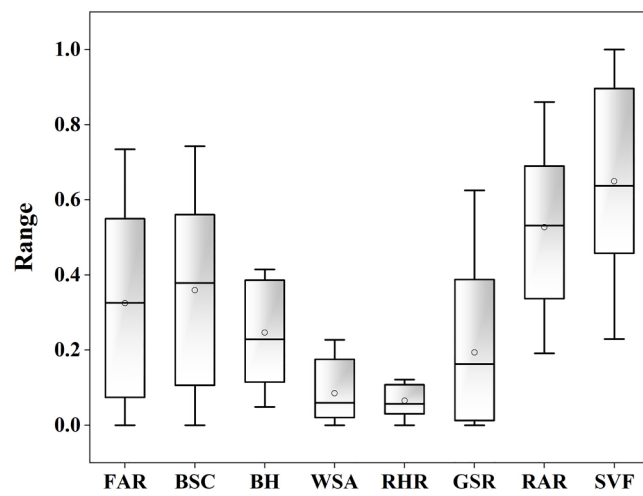


**Fig. 5.** Distribution of data on urban morphology influencing factors in the study area.

follows Eq. (1).

$$Y = \alpha + \beta_1 X_1 + \beta_2 X_2 + \dots + \beta_p X_p \quad (1)$$

where Y denotes the dependent variable,  $X_1, X_2, \dots, X_p$  denotes the independent variable,  $\beta$  denotes the regression coefficient, and  $\alpha$  denotes the constant term.

RF is an effective non-parametric model that is divided into RF classification and RF regression, and it can deal with complex nonlinear relationships (Peng, Yuan, Gao, Wang, & Chen, 2021; Xu et al., 2024). Considering the nonlinear relationship between complex urban elements, the RF model can be used to realize the nonlinear fitting of the influencing factors of the BEC. The specific data analysis steps are as follows: 1) Select 60 sample street blocks for correlation heat map analysis of neighborhood morphology influencing factors and BEC data for four seasons and the whole year. 2) Fit the influencing factors to the EUI by multiple regression. 3) Conduct the weight and energy consumption prediction analysis of each influencing factor concerning the BEC for the whole year using RF. 4) Apply the RF model to analyze the weights of the influence factors of subcategory street blocks and propose

recommendations for regulating the layout of street blocks to reduce the energy consumption of neighborhood buildings. In this research, RF regression was used to analyze the value of the contribution of the individual influencing factors to the BEC and predict the BEC, and each model included 800 decision trees with a maximum leaf depth of 10 and parameters such as the resulting correlation coefficients ( $R^2$ ) and the mean absolute error (MAE) were used to evaluate the predictive regression models (Antoniadis, Lambert-Lacroix & Poggi, 2021).

### 3. Results

#### 3.1. Regression of urban morphological indices and microclimate

This study was calculated based on the data shown in Appendix A. Fig. 7 shows the significance and Pearson's correlation analysis of urban morphology influencing factors and microclimate influencing factors for each season and throughout the year. Noticeably, for TEMP., differences in the influence factors exist in different seasons. Among them, the influence of BSC and SVF in spring was significant ( $p < 0.05$ ), with correlation coefficients of 0.33 and 0.28, respectively. The significant factors in summer were BSC, WSA, GSR, and SVF, with correlation coefficients of 0.73, 0.31, -0.54, and 0.29, respectively. The significant factors in autumn were BSC and SVF, with correlation coefficients of 0.49 and 0.30, respectively. The significant factors in winter were BSC, GSR, and SVF with correlation coefficients of 0.49, -0.34, and 0.27, respectively. Year-round significant factors were BSC, GSR, and SVF, with Pearson correlation coefficients of 0.55, -0.33, and 0.30, respectively.

For RH, the significance factors for spring were FAR (-0.65), BSC (-0.58), BH (-0.31), WSA (-0.74), RAR (-0.28), GSR (0.56), SVF (0.26), and RHR (-0.31). The significance factors for summer were FAR (-0.62), BSC (-0.66), BH (-0.29), WSA (-0.70), RAR (-0.33), GSR (0.64), and RHR (-0.31). The significance factors for autumn were FAR (-0.73), BSC (-0.51), BH (-0.40), WSA (-0.76), GSR (0.46), SVF (0.35), and RHR (-0.39). In contrast, the significance factors for winter were FAR (-0.84), BH (-0.49), WSA (-0.78), SVF (0.49), and RHR (-0.56). Finally, the significant factors throughout the year were FAR (-0.77), BSC (-0.44), BH (-0.42), WSA (-0.78), GSR (0.40), SVF (0.39), and RHR (-0.46).

For SR, the significance factors for spring were BSC (0.72), WSA (0.59), GSR (-0.47), and SVF (0.27). The significance factors for summer were BSC (0.73), WSA (0.56), GSR (-0.44), and SVF (0.27). The

**Table 2**  
Harbin building envelope restrictions.

Category	Coefficient of heat transfer $W/(m^2 \cdot K)$					Partition Wall or Floor between Non-heating Room
	Time	Form Factor	Roof	Wall	Window	
Residential buildings	1986 - 1995	0.30~≤0.32	0.512	0.628	2.6	1.136
	1996 - 2007	≤0.30	0.5	0.52	2.5	0.94
	2008 - 2018	≤0.28(6-11F)	0.3	0.4	2	0.8
	2018 - 2023	≤0.30	0.2	0.35	1.8	0.7
Public buildings	/	≤0.3	≤0.35	≤0.45	≤2.8(0.2<Window to Wall Ratio≤0.3) ≤2.5(0.3<Window to Wall Ratio≤0.4)	≤0.6

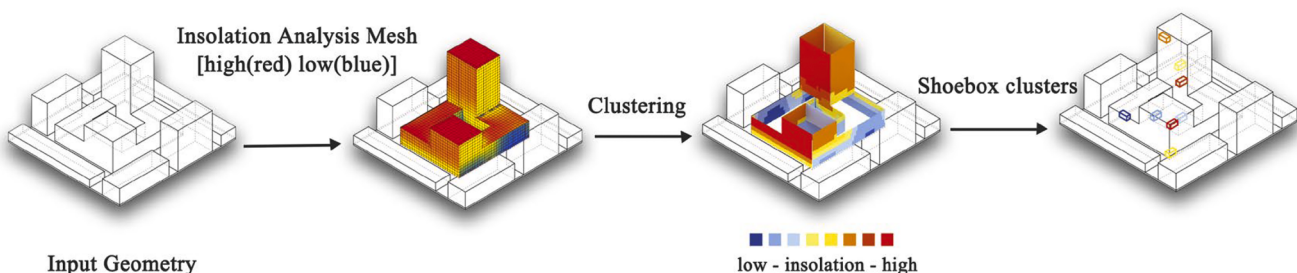


**Fig. 6.** modeling process theory (Dogan et al., 2017).

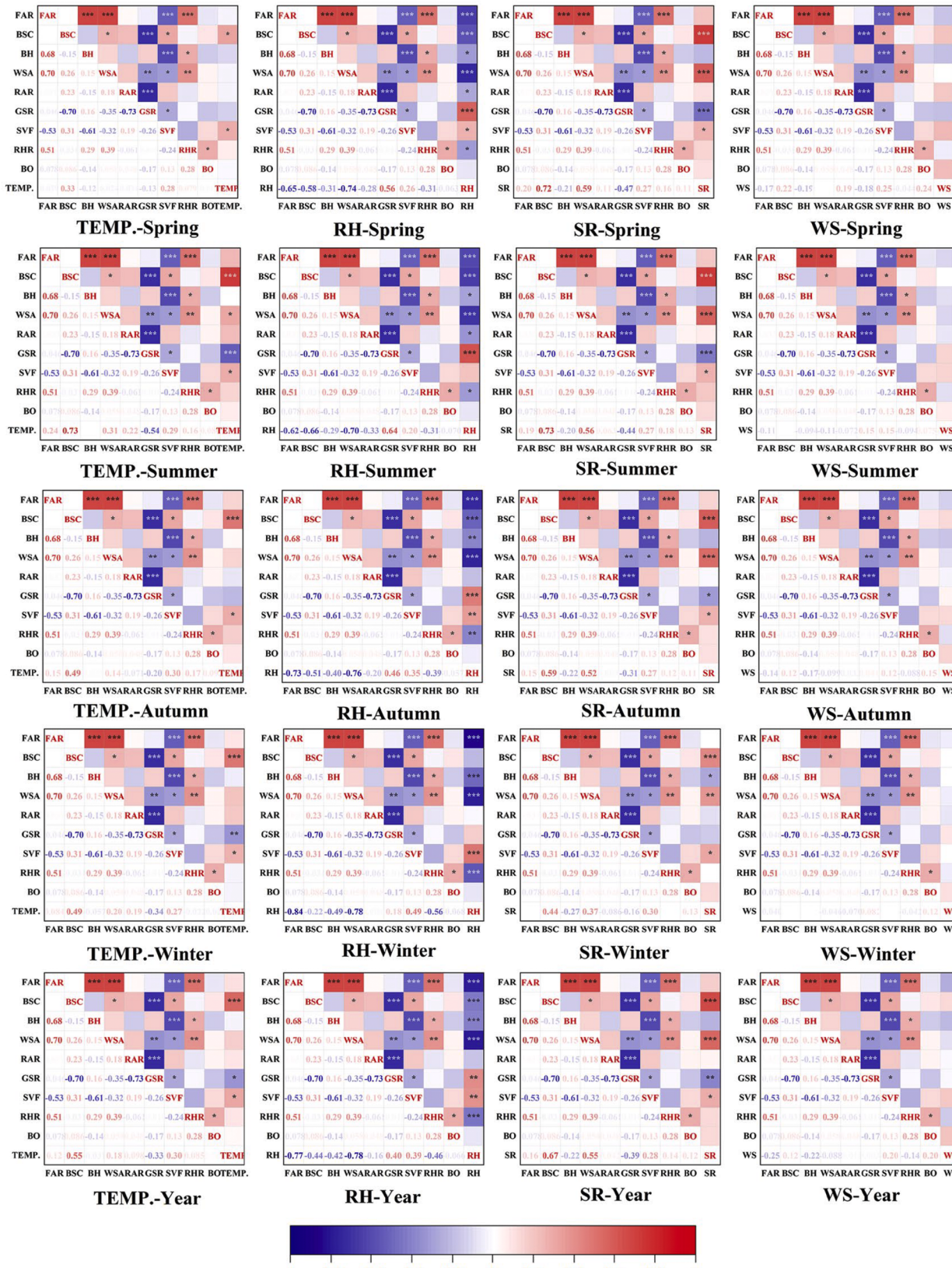


**Fig. 7.** Correlation analysis between urban morphology influences and microclimate

significant factors for autumn were BSC (0.59), WSA (0.52), GSR (-0.31), and SVF (0.27). The significance factors for winter were BSC (0.44), BH (-0.27), WSA (0.37), and SVF (0.30). Significance factors for the whole year were BSC (0.67), WSA (0.55), GSR (-0.39), and SVF (0.28).

### 3.2. Relationship between urban morphology, microclimate and energy consumption

#### 3.2.1. Single-factor analysis of each influence factor and the EUI

Fig. 8 shows the correlation analysis of the EUI of building clusters with urban morphology and microclimate influencing factors for each season in 60 sets of sample street blocks. Noticeably, BSC, GSR, SVF, TEMP., RH, and SR all have a significant effect on spring EUI ( $p < 0.05$ ), with Pearson correlation coefficients of 0.74, -0.50, 0.25, 0.26, -0.27 and 0.29, respectively. BSC, BH, GSR, TEMP., and RH had a significant effect ( $p < 0.05$ ) on summer EUI, with Pearson correlation coefficients of 0.65, 0.28, -0.43, 0.43, and -0.41, respectively. The FAR, BSC, GSR, SVF, TEMP., and SR all had a significant effect on autumn EUI ( $p < 0.05$ ), with Pearson correlation coefficients of -0.27, 0.72, -0.53, 0.32, 0.37, and 0.29, respectively. The significant factors on EUI in winter were FAR, BSC, BH, GSR, SVF, TEMP., RH, and SR with correlation coefficients of -0.59, 0.47, -0.51, -0.44, 0.52, 0.31, 0.33, and 0.43, respectively. BSC, RAR, GSR, SVF, TEMP., and SR had a significant effect ( $p < 0.05$ ) on EUI throughout the year, with correlation coefficients of 0.75, 0.26, -0.55, 0.34, 0.41, and 0.33, respectively. Overall, BSC, GSR, and TEMP. were significant for EUI in all seasons and throughout the year. In terms of Pearson's coefficients, the difference in Pearson's correlation coefficients between spring and autumn for each of the influencing factors was small, and the difference between summer and winter was large.

Combining Fig. 7 and Fig. 8, EUI is affected by a combination of urban morphology influencing factors and microclimate influencing factors. Throughout the year, urban morphology can directly affect EUI. Simultaneously, the urban morphology also alters the microclimate of the neighborhood, which in turn affects the EUI. For instance, the enhancement of BSC and SVF has a positive impact on TEMP., while the enhancement of BSC, SVF, and WSA promotes SR. Additionally, the enhancement of GSR decreases both TEMP. and SR. The increase in TEMP. and SR boosts EUI.

#### 3.2.2. Multiple linear regression of each influence factor and the EUI

As shown in Table 3, BSC, BH, RAR, and BO had a significant effect ( $p < 0.05$ ) on EUI during the transition season (spring and autumn), with beta values of 0.866, 0.370, 0.169, and 0.124 in spring, and 0.765, 0.636, 0.159, and 0.148 in autumn, respectively. Additionally, WSA had a significant effect ( $p < 0.05$ ) on spring EUI with a standardized coefficient of -0.475, and FAR with a standardized coefficient of -0.701. In summer, BSC, BH, WSA, and RAR significantly ( $p < 0.05$ ) affected EUI with standardized coefficients of 0.804, 0.498, -0.449, and 0.181. In winter, FAR, BSC, BH, WSA, and SVF had a significant effect ( $p < 0.05$ ) on EUI, with standardized coefficients of -1.399, 0.225, 0.542, 0.875, and 0.325, respectively. Throughout the year, FAR, BSC, BH, RAR, and BO had a significant effect ( $p < 0.05$ ) on EUI, with beta values of -0.651, 0.784, 0.584, 0.179, and 0.128.

Among the impact factors, some of the data have potential covariance issues because the urban morphology impact factor has both direct and indirect effects on the microclimate impact factor. In multiple regression models, the Variance Inflation Factor (VIF) can identify covariance in multiple regression equations, and a covariance problem

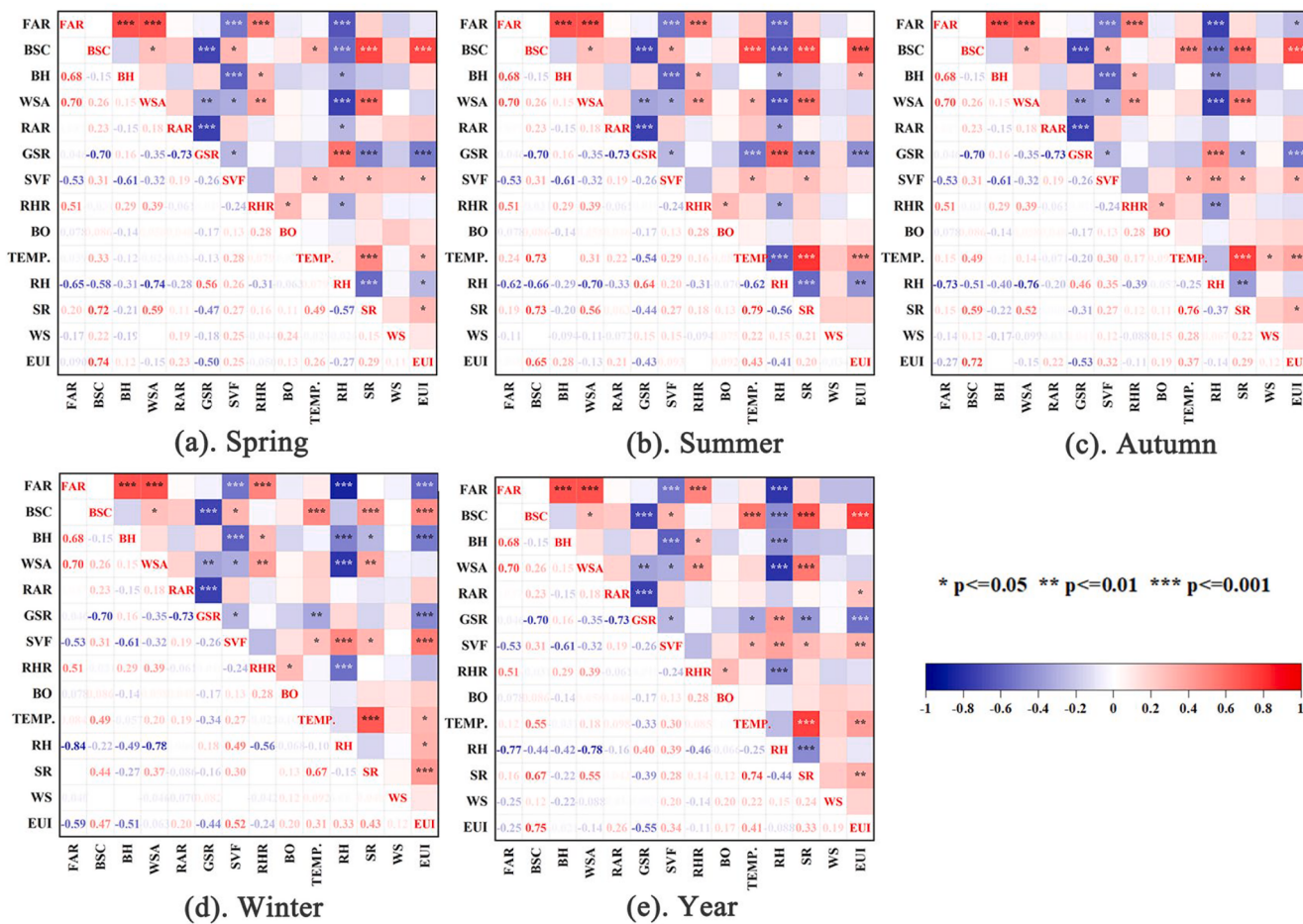


Fig. 8. Correlation analysis of EUI with urban morphology and microclimate impact factors.

**Table 3**

The results of multiple linear regression of each influence factor with EUI.

Category	Spring			Summer			Autumn			Winter			Sum		
	Beta	p	VIF												
Constant		0.015			0.016		0.028			0.332			0.172		
FAR	-0.063	0.663	5.866	0.023	0.888	5.840	-0.701	0.000	1.957	-1.399	0.000	5.964	-0.651	0.000	1.957
BSC	0.866	0.000	1.150	0.804	0.000	1.148	0.765	0.000	1.089	0.225	0.000	1.385	0.784	0.000	1.089
BH	0.370	0.000	1.112	0.498	0.000	1.091	0.636	0.000	2.048	0.542	0.000	3.886	0.584	0.000	2.048
WSA	-0.475	0.000	1.152	-0.449	0.000	1.148	0.016	0.888	3.453	0.875	0.005	3.920	-0.073	0.515	3.453
RAR	0.169	0.008	1.099	0.181	0.011	1.099	0.159	0.016	1.102	0.067	0.340	1.126	0.179	0.006	1.102
GSR	0.191	0.213	6.742	0.195	0.243	6.379	0.097	0.534	6.417	-0.105	0.282	2.205	0.180	0.238	6.417
SVF	0.026	0.761	2.097	-0.063	0.510	2.087	0.094	0.258	1.853	0.325	0.001	2.091	0.104	0.205	1.853
RHR	0.045	0.533	1.455	0.101	0.178	1.284	0.101	0.196	1.623	0.083	0.280	1.376	0.090	0.244	1.623
BO	0.124	0.042	1.029	0.114	0.087	1.029	0.148	0.020	1.025	0.060	0.369	1.041	0.128	0.039	1.025
TEMP.	0.022	0.731	1.156	-0.130	0.189	2.258	0.127	0.080	1.434	0.124	0.110	1.420	0.081	0.266	1.463
RH	0.237	0.068	4.876	0.066	0.685	6.070	0.171	0.209	4.949	-0.108	0.479	5.354	0.175	0.191	4.939
SR	-0.032	0.787	4.042	-0.158	0.230	3.955	0.136	0.126	2.123	0.113	0.179	1.640	0.040	0.682	2.639
WS	-0.075	0.239	1.150	-0.028	0.675	1.025	0.018	0.782	1.067	0.089	0.174	1.006	0.041	0.523	1.122

exists when VIF > 5 (Akinwande, Dikko & Samson, 2015). To address the impact of covariance on the multiple regression equation, stepwise regression is a more effective approach. Consequently, the multiple regression equation excludes the influencing factors with VIF > 5 and  $p > 0.05$ , as illustrated in Eqs. (2)-(6).

$$\begin{aligned} EUI_{\text{Spring}} = & 1.109 \times BSC + 0.536 \times BH - 0.597 \times WSA + 0.241 \\ & \times RAR + 0.135 \times BO - 0.191 \end{aligned} \quad (\text{Eq2})$$

$$(R^2 = 0.813 \ p < 0.001 \ F = 47.016)$$

$$\begin{aligned} EUI_{\text{Summer}} = & 1.139 \times BSC + 0.798 \times BH - 0.624 \times WSA + 0.286 \\ & \times RAR - 0.213 \end{aligned} \quad (\text{Eq3})$$

$$(R^2 = 0.763 \ p < 0.001 \ F = 44.291)$$

$$\begin{aligned} EUI_{\text{Autumn}} = & -0.782 \times FAR + 0.798 \times BSC + 0.750 \times BH + 0.185 \\ & \times RAR + 0.131 \times BO - 0.068 \end{aligned} \quad (\text{Eq4})$$

$$\begin{aligned} EUI_{\text{Winter}} = & 0.638 \times BH + 0.893 \times WSA + 0.234 \times BSC + 0.322 \\ & \times SVF \end{aligned} \quad (\text{Eq5})$$

$$(R^2 = 0.770 \ p < 0.001 \ F = 36.180)$$

$$\begin{aligned} EUI_{\text{year}} = & 0.808 \times BSC + 0.681 \times BH - 0.717 \times FAR + 0.205 \times RAR \\ & + 0.112 \times BO \end{aligned} \quad (\text{Eq6})$$

$$(R^2 = 0.806 \ p < 0.001 \ F = 44.915)$$

The impact of each influencing factor on the change of EUI in four seasons and throughout the year is illustrated in Eqs. 2–6. The calculations reveal variations in the influencing factors of urban morphology on EUI across different climatic conditions in the four seasons. When considering the entire year, a 10 % increase in BSC, BH, RAR, and BO results in EUI increases of 8.08 %, 6.81 %, 2.05 %, and 1.12 % respectively. Additionally, for every 10 % increase in FAR, the EUI decreases by 7.17 %.

### 3.3. Weight analysis of individual impact factors and energy consumption prediction of building cluster

RF was used to reduce the more complex nonlinear relationships that exist in the building cluster energy consumption by each influencing factor. The BEC was used as the independent variable, and the urban morphology and microclimate influencing factors were used as the dependent variables. An increase in the number of decision trees in the RF improves the goodness of fit ( $R^2$ ) of the training set as well as the test set, but too many decision trees can lead to data overfitting. To obtain better fitting performance, after several test iterations, the RF regression model node splitting was evaluated with the MSE criteria, the number of decision trees was set to 800, the maximum tree depth was 10, and the maximum number of leaf nodes was 50.

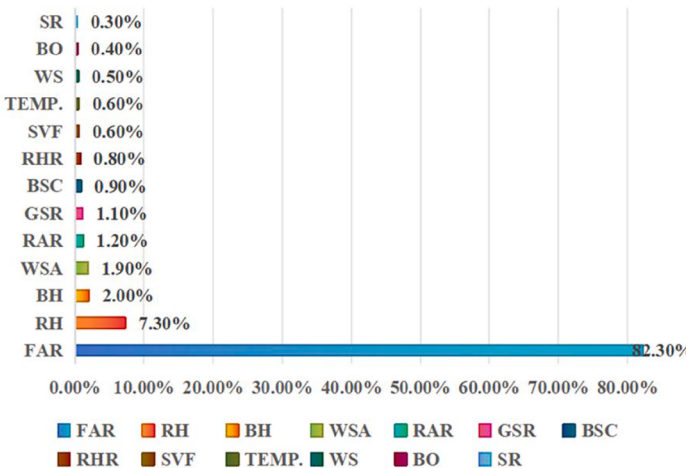
The RF model can explain and rank the contribution of the dependent variable to the variables, which is very important for influencing the weight distribution of the factors and making the prediction of the energy consumption of building clusters. Fig. 9 shows the contribution and correlation analysis of urban morphology and microclimate influencing factors to the total energy consumption of building clusters throughout the year. As shown in Fig. 9(a), the contribution of each influence factor from high to low was FAR (82.30 %), RH (7.30 %), BH (2.00 %), WSA (1.90 %), RAR (1.20 %), GSR (1.10 %), BSC (0.90 %), RHR (0.80 %), SVF (0.60 %), TEMP.(0.60 %), WS (0.50 %), BO (0.40 %), and SR (0.30 %). Noticeably, FAR contributed the most to the energy consumption of building clusters and played an extremely important role in the construction of the RF prediction model.

Table 4 lists the result parameters of the RF regression model test set, training set, and sample prediction. Noticeably, the sample prediction  $R^2$  was 0.944, the MAPE was 4.331, and the model fit was good. Fig. 10 shows the analysis of the predicted and simulated values of the total energy consumption of building clusters. Noticeably, from the perspective of block type, the simulated and predicted energy consumption of residential building blocks (1–30 in Fig. 10) in all seasons has a smaller error, and the simulated and predicted energy consumption of public building blocks, such as commercial and office (31–60 in Fig. 10), has a larger error. This is attributable to the electricity consumption of public building blocks, such as office and commercial, being influenced to a greater extent by the subjective energy use behavior than that of residential building blocks.

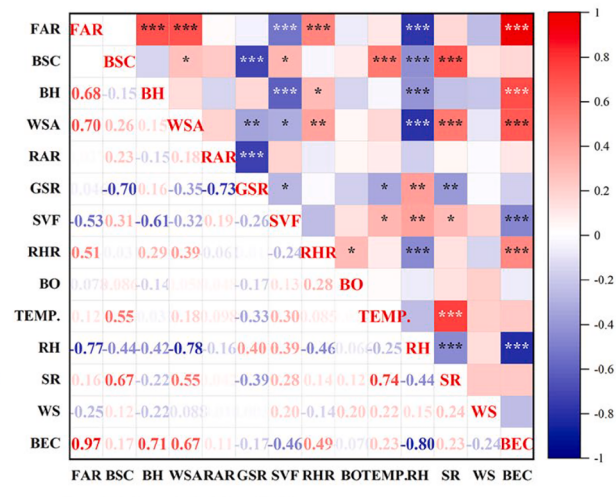
## 4. Discussion

### 4.1. Research contributions and limitations

Table 5 presents a selection of studies conducted in various climate zones in recent years. Based on research areas and content, the majority of scholars have concentrated their research efforts in the C Köppen



(a). The weight value of each influence factor



(b). Correction analysis of each influence factor

Fig. 9. Contribution value and correlation analysis of each influence factor to the BEC.

**Table 4**  
Random forest test set and predicted outcome parameters.

Item	MSE	RMSE	MAE	MAPE	R <sup>2</sup>
Training Set	2078,221,194,369.325	1,441,603.688	957,922.713	3.092	0.985
Test set	18,730,168,556,678.555	4,327,836.475	2862,770.993	7.14	0.834
Sample prediction	7380,529,057,715.114	2,716,712.914	1547,841.981	4.331	0.944

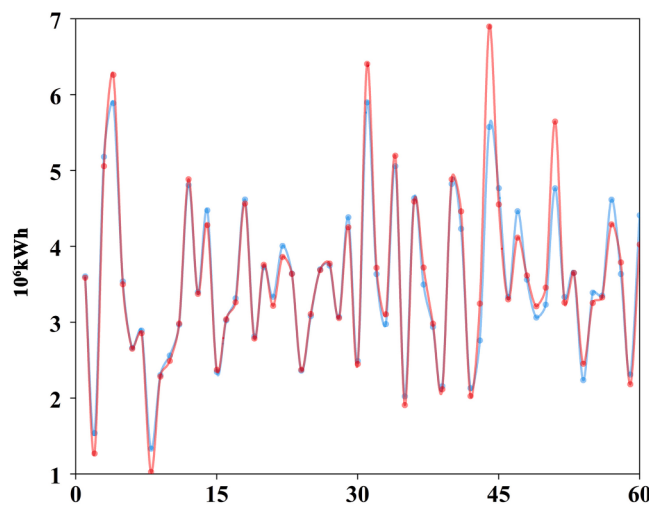


Fig. 10. Comparison of predicted and simulated values.

climate zone. In colder regions, the emphasis lied on studying heating energy consumption, whereas in warmer regions, scholars prioritized investigating cooling energy consumption. Additionally, research on cooling energy consumption in the Dwa climate zone is relatively limited.

BEC has relied on simulation methods, with EnergyPlus being the most widely used software. However, EnergyPlus is more suitable for simulating the energy consumption of a single building. The energy simulation approach adopted in this paper is UMI, which utilizes the principle of "shoebox" to better consider the impact of various factors on the energy consumption of building clusters. The majority of scholars typically use regression analysis for their data analysis. However, both correlation analysis and regression analysis predominantly focus on

linear relationships. For instance, scholars (Leng et al., 2020; Liu et al., 2023; Xu et al., 2023) have selected different influencing factors in their studies, largely due to the varying focuses of their research. Generally, in regression analysis, EUI shows a significant correlation with building density, which is consistent with our findings. However, the research also confirmed that BO and RAR significantly impact the EUI of neighborhood building clusters. Furthermore, several influencing factors have a non-linear effect on the energy consumption of building clusters. Therefore, the research proposed that combining regression analysis with RF analysis can provide a more comprehensive investigation into the impact of urban morphology and microclimate on the energy consumption of building clusters.

Morphology parameters affecting EUI vary across different climatic zones. In the subtropics, FAR was typically positively correlated with EUI; however, it was negatively correlated in this research. This is attributed to the long and cold winters in the study area, where building clusters are predominantly arranged in a centralized layout. The blocks in the research area utilize a centralized hot water heating system, facilitating heat transfer within the internal units. Although the increase in FAR results in a rise in total energy consumption, EUI is not as significant as BEC due to the expansion of the total floor area. Thus, the research confirms the substantial impact of climate context and building layout on energy consumption.

The research developed a regression equation of urban morphology influences and microclimate influences on EUI. The equation not only considered the influence of neighborhood microclimate on the energy consumption of building clusters but also accounted for the seasonal variations in these impacts on the energy consumption of building clusters. The research experimentally analyzed the energy consumption of building clusters and determined the weight of each influencing factor using the RF model. This not only demonstrated the significant role of FAR in the energy consumption of building clusters in severe cold regions but also confirmed the efficacy of using the RF model to predict the influence of urban morphology and microclimate on the total energy

**Table 5**

Neighborhood morphology and building energy consumption study tables.

Research site	Köppen climate zone classification and research content	Method	Related Conclusions	Impact Factor (+: positive correlation (-: negative correlation)
Harbin (The paper)	Dwa Total EUI	UMI+UWG+ MLR+RF	TEMP. and SR were positively correlated with building EUI in building clusters. BSC, BH, RAR, and BO were positively correlated with EUI. FAR was positively correlated with BEC and negatively correlated with RH. The contribution rates were 82.3 % and 7.3 %, respectively.	BSC(+), BH(+), BO(+), RAR(+), TEMP.(+), RH (+), FAR(-)
Harbin China (Leng et al., 2020)	Dwa The heating load EUI	EnergyPlus+GIS+Correlation Analysis	Greater BSC, FAR, BH, RHR, WSA, and lower GSR are beneficial to the reduction of heating energy consumption. FAR is the most critical factor in saving heating energy by up to 10.82 kWh/m <sup>2</sup> /y, with the addition of one more unit.	GSR(+), FAR(-), BSC(-), BH(-), RHR(-), WSA(-)
Jianhu China (Liu et al., 2023)	Cfa Total EUI	Grasshopper platform+Wallacei X+Correlation Analysis	BD, OSR, SC and, PAR have significant correlations with the total building energy use intensity of the block. The building shape and site coverage ratio have significant effects on energy consumption. The more complex the shape, the higher the energy consumption of the building. Studies in different climates have shown that higher building compactness improves building energy efficiency.	BSC(+), OSR(+), PAR (+), SC(+), FAR(-), AF(average number of floors)(-) SD (staggered degree)(-)
Nanjing China (Zhang & Gao, 2021)	Cfa Cooling and heating loads EUI	ENVI-Met+EnergyPlus+Correlation and regression analyses	Air temperature and direct shortwave radiation are negatively correlated with the SAR. The cooling and heating loads are negatively correlated with the FAR and SAR, and positively correlated with the mean SVF. The differences in energy loads can reach 23.4 % with an obvious deviation of the regression analyses of hourly heating loads and air temperature if neglecting the microclimate effect.	FAR(-), rOSR(-), SAR(-) SVF(+), Cooling load: T(+) RH(-) Heating load: T(+) RH(-)
Abu Dhabi (Mirkovic & Alawadi, 2017)	Bwh Cooling load	EnergyPlus (Honeybee)	Urban density can enhance energy performance and decrease solar heat gain by increasing energy density. Buildings are optimally organized in the long run, providing more shading and passively reducing cooling needs.	BSC(+)
Shanghai (Wang et al., 2022)	Cfa Cooling and heating loads EUI	EnergyPlus+data-driven enhanced global sensitivity analysis (GSA)	The urban morphology factors representing buildings' geometric characteristics tend to have greater impacts on energy performance, among which the top influencing factors are relative compactness, building coverage ratio, and building height distribution.	Heating load: FAR(+), BSC(+) REC(-), BH(-) Cooling load: BH(+), FAR(+) BSC(-), REC(-)
Wuhan (Xu et al., 2023)	Cfa Cooling and heating loads EUI	EnergyPlus+MLR	Regression modeling was carried out, and the study concluded that the EUI of residential blocks was mainly affected by shape factor, building density, and floor area ratio, while EUI-PV and PSR were mainly affected by height and sky view factor.	SF(+), FAR(+) BD(-)

consumption of building clusters, with a goodness-of-fit of 0.944 ( $R^2$ ). These findings provide a robust foundation for predicting energy consumption at the urban scale in cold regions and other large-scale building complexes. They offer theoretical support for predicting the energy consumption of building complexes at the urban scale in cold regions and other large scales.

The limitations of this research are: 1) The conclusions of this research apply to the severe cold region, and its applicability to other climatic zones or special building layouts is yet to be verified. 2) This research does not consider the effects of some variable factors, such as traffic flow, bodies of water and human-induced accidental energy use, on the energy consumption of building clusters. Therefore, future studies will incorporate more non-morphological factors that may affect the energy consumption of building clusters.

#### 4.2. Strategies to mitigate energy consumption in the central city area

To provide targeted recommendations for reducing cluster energy consumption, this section analyzes the percentage contribution of each influencing factor to cluster energy consumption for each of the four types of street blocks. The contribution of each influencing factor to the energy consumption of building clusters as obtained through the RF

regression prediction analysis of the annual energy consumption of building clusters in different types of street blocks and the influencing factors is shown in Fig. 11.

The most important factors influencing the BEC for new residential building street blocks were the urban morphology indicator WSA (15.8 %), and the microclimate indicator RH (17.1 %), with WSA being positively correlated and RH being negatively correlated as shown in Fig. 9(b). For RH, the urban morphology influence factor WSA had the greatest impact on RH and was negatively correlated. For the old residential building street blocks, the urban morphology indicators FAR (17.5 %) and the microclimate indicator RH (15.6 %) were the most important factors affecting BEC. Further, BEC was positively correlated with FAR, negatively correlated with RH, and FAR was negatively correlated with RH. In commercial street blocks, urban morphology indicators FAR (28.2 %) and BH (15.4 %) had the greatest influence on BEC, and both were positively correlated with BEC. The urban morphology indicator FAR (18.3 %) and microclimate indicator RH (15.5 %) were the most important factors affecting BEC in office building street blocks. FAR was positively correlated with BEC and negatively correlated with RH, whereas FAR was negatively correlated with RH.

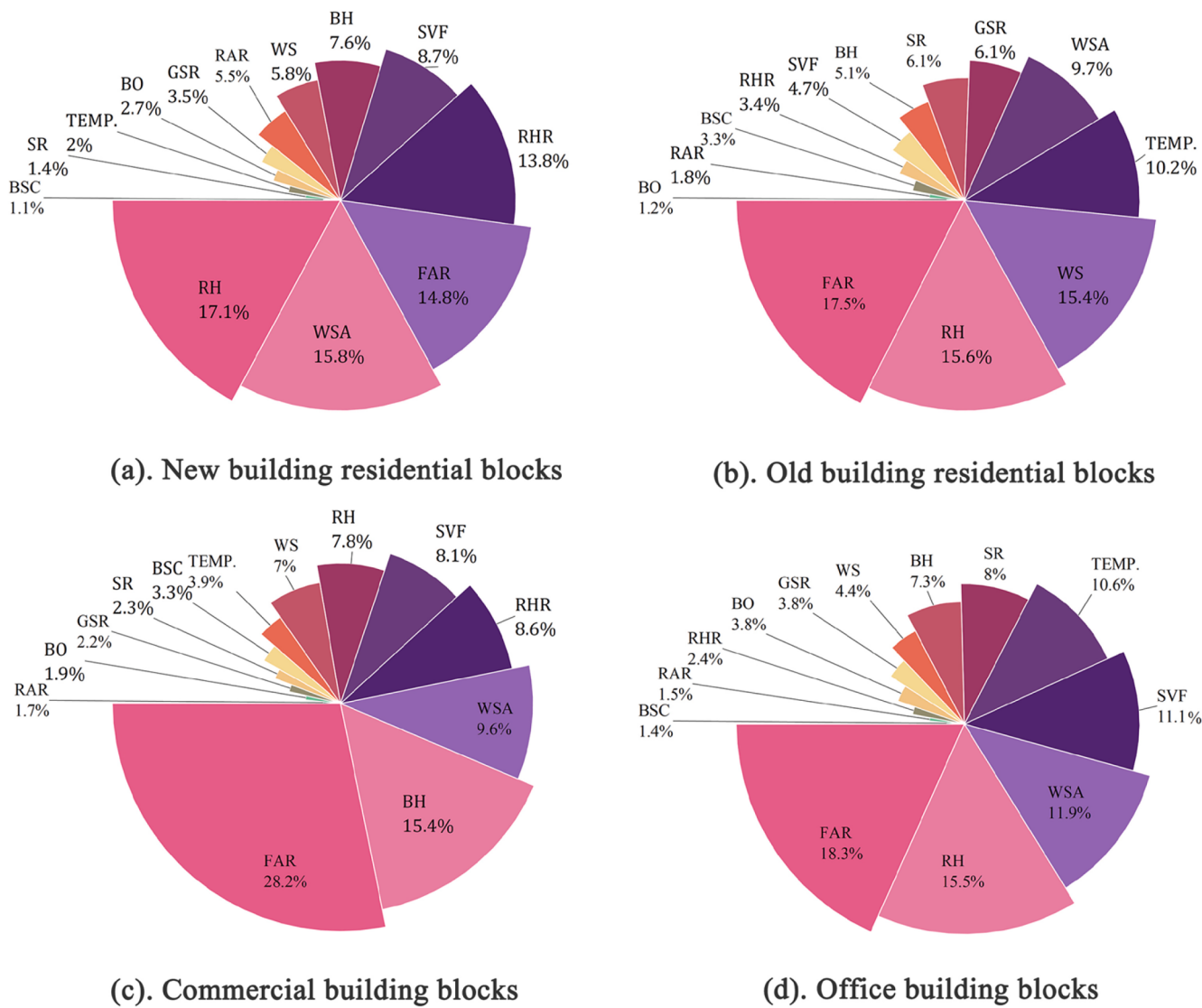


Fig. 11. Comparative analysis of the contribution of building energy consumption impact factors in four types of street blocks.

#### 4.3. Energy efficiency optimization strategies for building clusters

The following urban neighborhood planning and construction strategies are proposed to reduce the energy consumption of urban building complexes in cold regions under the premise of keeping the intensity of land use (FAR, Site area) unchanged. New residential blocks should increase the RH of the community through increasing GSR and building interval. For old residential blocks, block layout should consider reducing the BH, BSC, WSA, and RHR and increasing SVF and GSR to raise RH with conditions permit. For commercial blocks, it is crucial to reduce the BH, and it is also necessary to appropriately increase the building base area and optimize the heat dissipation of the building facades. In general, office buildings are usually high-rise with large base areas, energy conservation can be achieved by adjusting the heat dissipation of building facades and increasing building interval and GSR.

According to the annual multiple regression equation, EUI can be reduced by increasing FAR, decreasing BSC, BH, and RAR, and adjusting the block layout towards a direction with a smaller angle to the north can further reduce energy consumption effectively. As shown in Fig. 9 (b), the increase in RH leads to a decrease in BEC. So the annual BEC can be reduced by decreasing BSC, BH, WSA, and RHR, and increasing GSR and SVF to enhance RH in the community.

To test the strategy, sample 19 was selected for rearrangement. As

depicted in Fig. 12, the building layout was reorganized without changing the FAR and keeping the original building texture. The average height was reduced by 6.3 %, the GSR was increased from 17 % to 33 %, the building interval was enlarged from 13 m to 18 m, and the base area of buildings was increased from 39,597.m<sup>2</sup> to 40,118 m<sup>2</sup>. The test results indicate that the EUI of the adjusted layout is 122 kWh/m<sup>2</sup> and the BEC is 26,676,604 kWh, representing a 4.1 % decrease in EUI and a 4.3 % decrease in BEC per year. To achieve maximum energy savings within a quantifiable range, a multi-objective optimization algorithm can be employed based on the quantitative relationship between each element and energy consumption proposed in the research.

#### 5. Conclusion

This study was based on urban multi-source data and employed 60 actual street blocks in Harbin, a typical city in a cold climate, as a case study. It extracted and calculates urban morphology and microclimate influencing factors at the neighborhood level by combining measurement and simulation methods. The study established datasets on building cluster energy consumption that incorporates neighborhood morphology and microclimate. After data preprocessing, the building cluster energy consumption was analyzed and predicted, and the following were the main conclusions drawn:

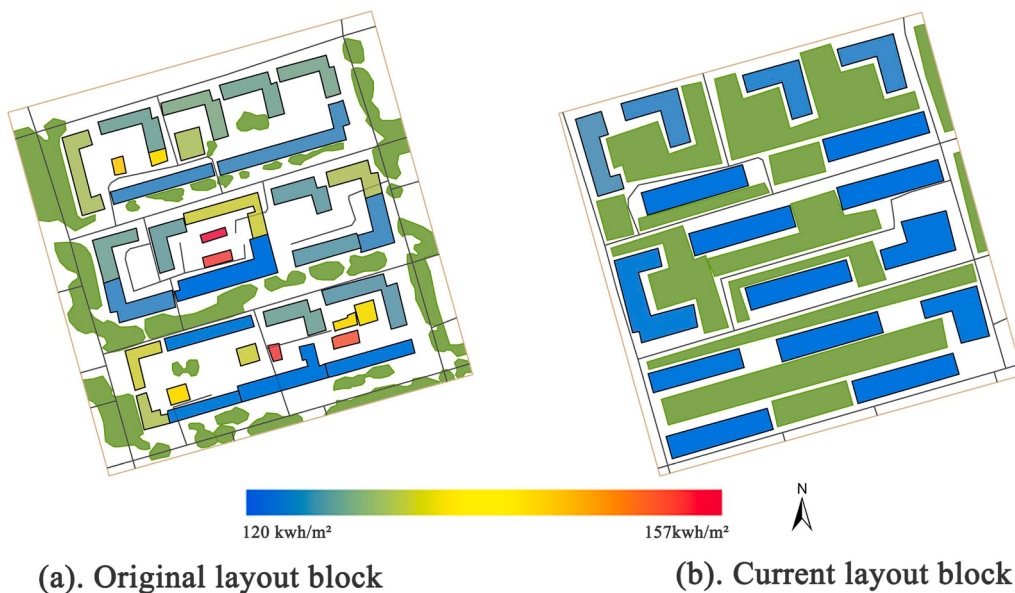


**Fig. 12.** Neighborhood adjustment energy distribution map.

- (1) The impact of urban morphology on microclimate and vice versa on energy use intensity varies according to season. Annual TEMP. and SR was significantly correlated with EUI, whereas RH and WS exhibited no significant correlation with EUI. In addition, RH exhibited a significant negative correlation with the BEC of neighborhood building clusters.
  - (2) Multiple linear regression equations were proposed for urban morphology, microclimate influencing factors, and EUI. The influencing factors that significantly affected EUI varied from season to season. Throughout the year, EUI showed significant correlations with BSC, BH, FAR, BO, and RAR.
  - (3) FAR was the most important factor and contributed 82.3 % to the BEC of the building cluster in all four seasons.
  - (4) The research explored and discussed the influence of various factors in different street blocks on the energy consumption of building clusters in cold regions. Based on the analysis results, the research put forward suggestions on the building layouts of reducing building cluster energy consumption from the perspectives of EUI and BEC.

This research is of great significance for the planning of cold urban street blocks to reduce the energy consumption of buildings and clusters, lower urban energy consumption, and enhance the level of urban low-carbon development.

## Appendix A

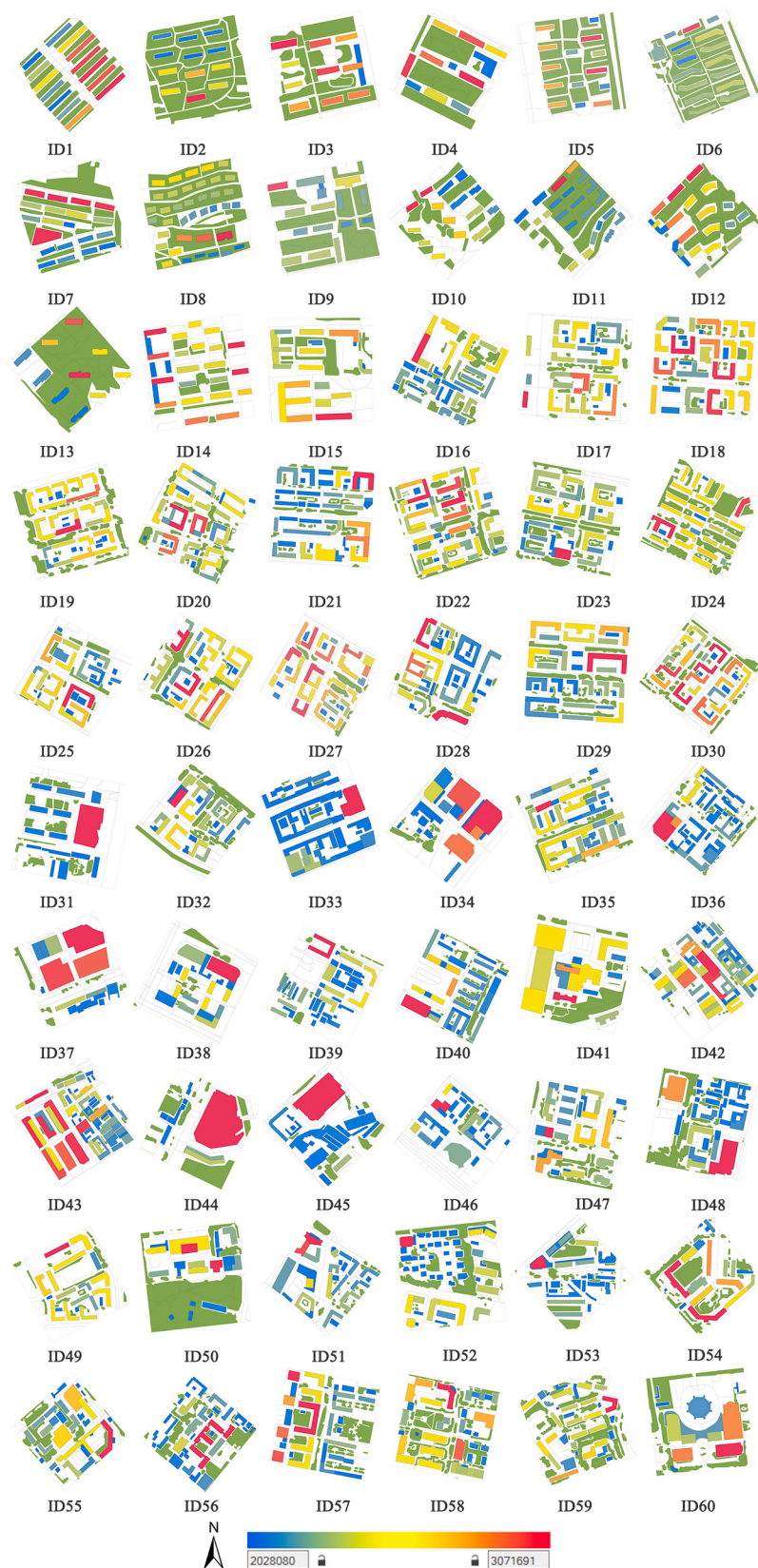
Item	ID	FAR	BSC	BH (m)	WSA (10 <sup>5</sup> m <sup>2</sup> )	RAR	GSR	SVF	RHR	BO (°)	EUI (kWh/m <sup>2</sup> )				
											Spring	Summer	Autumn	Winter	Sum
New building residential blocks	1	1.88	0.27	20.55	1.45	0.42	0.31	0.79	0.32	48.0	22.02	21.94	25.58	49.88	119.43
	2	0.67	0.11	18.00	0.6	0.22	0.67	0.84	0.66	80.0	22.01	22.16	25.61	48.40	118.18
	3	2.77	0.15	54.86	1.64	0.27	0.38	0.66	0.66	79.0	21.48	22.06	24.71	45.91	114.16
	4	3.46	0.20	52.53	1.88	0.17	0.43	0.72	1.67	116.0	21.57	21.99	24.45	45.05	113.06
	5	1.83	0.10	57.00	1.43	0.40	0.40	0.71	0.59	83.0	21.66	22.69	25.94	49.56	119.86
	6	1.37	0.19	22.16	1.21	0.29	0.43	0.82	0.18	67.0	22.27	23.07	26.12	49.67	121.13
	7	1.50	0.20	19.27	1.24	0.35	0.36	0.81	2.43	73.0	22.51	22.70	25.61	48.00	118.82
	8	0.48	0.24	6.00	0.69	0.21	0.44	0.93	2.02	79.0	24.44	21.11	28.52	59.04	133.10
	9	1.23	0.22	19.79	0.87	0.26	0.43	0.80	2.08	80.0	21.83	21.72	25.12	47.74	116.41
	10	1.33	0.15	28.63	1.0	0.58	0.28	0.75	0.45	47.0	21.53	22.28	25.21	47.63	116.65

*(continued on next page)*

(continued)

Item	ID	FAR	BSC	BH (m)	WSA (10 <sup>5</sup> m <sup>2</sup> )	RAR	GSR	SVF	RHR	BO (°)	EUI (kWh/m <sup>2</sup> )				
											Spring	Summer	Autumn	Winter	Sum
Old building residential blocks	11	1.57	0.19	24.73	1.26	0.38	0.43	0.77	0.73	45.0	21.75	22.34	25.40	49.16	118.66
	12	2.61	0.22	34.54	1.72	0.38	0.39	0.76	0.56	47.0	21.87	21.98	25.19	48.10	117.14
	13	1.83	0.12	46.24	1.2	0.02	0.66	0.69	0.22	50.0	21.59	22.08	24.96	46.72	115.35
	14	2.27	0.22	30.58	1.74	0.58	0.09	0.68	0.65	82.0	21.91	22.61	25.46	47.71	117.70
	15	1.15	0.23	16.68	1.07	0.56	0.11	0.87	0.40	90.0	24.08	23.62	27.31	53.49	128.49
	16	1.49	0.32	13.86	1.38	0.46	0.12	0.83	0.37	115.0	23.91	24.63	26.80	52.05	127.38
	17	1.64	0.25	19.86	1.49	0.60	0.06	0.83	0.44	93.0	22.59	22.38	26.63	53.09	124.68
	18	2.33	0.36	19.12	1.93	0.47	0.06	0.81	0.78	93.0	22.55	22.05	26.18	51.74	122.52
	19	1.37	0.25	17.26	1.38	0.48	0.17	0.82	0.47	75.0	23.14	22.36	27.10	54.49	127.10
	20	1.83	0.29	18.89	1.72	0.60	0.11	0.81	0.61	117.0	23.45	22.80	27.25	54.56	128.07
	21	1.62	0.34	14.38	1.55	0.58	0.09	0.88	0.47	93.0	23.08	22.65	26.46	51.96	124.15
	22	1.94	0.31	18.47	1.78	0.43	0.16	0.87	0.44	72.0	22.83	22.11	26.61	53.15	124.70
	23	1.89	0.27	21.33	1.52	0.35	0.18	0.81	0.58	100.0	22.32	21.90	25.77	50.32	120.31
	24	1.18	0.22	15.77	1.20	0.29	0.29	0.83	0.77	115.0	22.78	22.41	26.72	53.57	125.48
	25	1.56	0.27	16.99	1.43	0.47	0.06	0.85	0.48	120.0	22.90	22.07	26.62	53.34	124.93
	26	1.81	0.32	17.25	1.64	0.49	0.09	0.86	0.59	29.0	23.38	22.76	27.01	54.01	127.17
	27	1.85	0.29	19.52	1.73	0.56	0.06	0.82	0.54	30.0	23.03	22.32	27.07	55.01	127.43
Commercial building blocks	28	1.51	0.34	13.47	1.51	0.51	0.05	0.88	0.42	27.0	23.09	21.97	26.86	54.34	126.26
	29	2.17	0.36	17.98	1.87	0.31	0.13	0.79	0.38	92.0	22.65	22.20	26.17	51.22	122.23
	30	1.20	0.22	14.96	1.28	0.45	0.13	0.82	0.42	39.0	23.02	22.47	27.13	55.45	128.08
	31	3.10	0.20	46.75	1.44	0.69	0.11	0.84	0.89	100.0	25.77	29.62	27.54	46.36	129.30
	32	1.81	0.25	32.01	1.43	0.56	0.19	0.68	0.44	40.0	24.29	25.36	27.06	51.80	128.52
	33	1.29	0.49	19.46	1.36	0.40	0.02	0.85	0.28	70.0	29.63	34.67	30.98	54.62	149.90
	34	2.31	0.39	54.92	1.26	0.47	0.04	0.71	0.55	40.0	28.55	34.23	29.22	48.31	140.32
	35	0.77	0.36	12.87	1.02	0.46	0.09	0.88	0.20	69.0	30.07	34.78	31.98	58.48	155.31
	36	2.12	0.33	34.87	1.59	0.41	0.06	0.80	0.51	130.0	26.37	29.32	28.35	51.41	135.45
	37	1.62	0.40	43.36	1.10	0.36	0.04	0.77	0.34	65.0	29.00	34.35	29.82	50.03	143.19
	38	1.47	0.24	31.23	1.13	0.51	0.05	0.84	0.17	115.0	23.88	25.21	26.88	50.66	126.63
	39	0.97	0.27	17.17	1.09	0.50	0.03	0.85	0.97	115.0	25.47	27.55	28.65	54.15	135.82
	40	2.25	0.34	36.79	1.72	0.48	0.09	0.79	0.93	116.0	26.36	29.68	28.51	51.03	135.59
	41	1.96	0.38	32.21	1.43	0.36	0.17	0.74	1.32	102.0	28.30	33.30	29.72	50.98	142.29
	42	0.82	0.41	12.00	1.11	0.57	0.02	0.90	0.36	141.0	30.02	33.87	31.79	59.03	154.71
	43	1.27	0.45	17.84	1.52	0.52	0.03	0.85	0.47	141.0	30.62	35.54	32.55	60.68	159.38
Office building blocks	44	3.04	0.31	84.14	1.31	0.48	0.21	0.83	0.68	26.0	28.84	34.26	29.60	49.17	141.87
	45	2.07	0.39	51.18	1.27	0.45	0.07	0.81	0.34	48.0	27.31	31.52	28.76	50.06	137.65
	46	1.62	0.24	20.06	1.29	0.74	0.02	0.85	0.62	130.0	24.74	26.22	26.52	49.64	127.12
	47	2.04	0.29	21.41	1.52	0.60	0.11	0.83	0.76	101.0	24.63	26.29	26.29	48.72	125.93
	48	1.78	0.33	16.41	1.29	0.50	0.18	0.87	0.25	11.0	25.23	27.48	26.38	47.96	127.04
	49	1.59	0.22	21.92	1.31	0.71	0.07	0.80	0.41	64.0	23.84	24.68	26.54	51.00	126.07
	50	1.72	0.20	25.25	1.12	0.33	0.46	0.84	0.20	84.0	25.11	27.84	26.02	46.27	125.24
	51	2.68	0.31	25.66	1.96	0.64	0.05	0.74	0.54	40.0	25.87	29.16	27.30	49.33	131.66
	52	1.61	0.25	19.86	1.41	0.46	0.19	0.83	0.45	84.0	23.85	24.44	26.75	51.35	126.39
	53	1.86	0.26	22.05	1.45	0.50	0.14	0.82	0.57	49.0	23.34	23.91	26.14	49.13	122.52
	54	1.17	0.24	14.97	1.01	0.44	0.22	0.88	0.61	50.0	25.45	27.70	27.09	50.61	130.84
	55	1.61	0.34	14.42	1.35	0.41	0.15	0.85	0.59	50.0	24.51	25.35	26.46	50.32	126.65
	56	1.61	0.32	15.21	1.45	0.38	0.20	0.88	0.51	40.0	24.82	26.39	26.76	50.80	128.78
	57	2.14	0.30	22.03	1.65	0.30	0.20	0.88	1.18	100.0	23.98	24.78	26.41	49.89	125.06
	58	1.83	0.33	17.18	1.47	0.44	0.23	0.80	0.50	102.0	25.46	27.54	26.78	49.63	129.41
	59	1.07	0.22	14.74	1.10	0.55	0.23	0.88	0.20	71.0	23.98	25.04	26.92	51.92	127.85
	60	2.05	0.28	21.45	1.03	0.52	0.20	0.84	0.57	84.0	24.74	26.81	25.57	45.41	122.53

**Appendix B**



## References

- Ahmad, M. W., Mourshed, M., & Rezgui, Y. (2017). Trees vs Neurons: Comparison between random forest and ANN for high-resolution prediction of building energy consumption. *Energy and buildings*, 147, 77–89. <https://doi.org/10.1016/j.enbuild.2017.04.038>
- Ahn, Y., & Sohn, D. W. (2019). The effect of neighbourhood-level urban form on residential building energy use: A GIS-based model using building energy benchmarking data in Seattle. *Energy and Buildings*, 196, 124–133. <https://doi.org/10.1016/j.enbuild.2019.05.018>
- Akinwande, M. O., Dikko, H. G., & Samson, A. (2015). Variance inflation factor: As a condition for the inclusion of suppressor variable(s) in regression analysis. *Open Journal of Statistics*, 5(07), 754. <https://doi.org/10.4236/ojs.2015.50705>
- Antoniadis, A., Lambert-Lacroix, S., & Poggi, J. M. (2021). Random forests for global sensitivity analysis: A selective review. *Reliability Engineering & System Safety*, 206, Article 107312. <https://doi.org/10.1016/j.ress.2020.107312>
- Boccalatte, A., Fossa, M., Gaillard, L., & Menezo, C. (2020). Microclimate and urban morphology effects on building energy demand in different European cities. *Energy and Buildings*, 224, Article 110129. <https://doi.org/10.1016/j.enbuild.2020.110129>
- Bourdeau, M., qiang Zhai, X., Nefzaoui, E., Guo, X., & Chatellier, P. (2019). Modeling and forecasting building energy consumption: A review of data-driven techniques. *Sustainable Cities and Society*, 48, Article 101533. <https://doi.org/10.1016/j.scs.2019.101533>
- Bueno, B., Norford, L., Hidalgo, J., & Pigeon, G. (2013). The urban weather generator. *Journal of Building Performance Simulation*, 6(4), 269–281. <https://doi.org/10.1080/19401493.2012.718797>
- Bueno, B., Roth, M., Norford, L., & Li, R. (2014). Computationally efficient prediction of canopy level urban air temperature at the neighbourhood scale. *Urban Climate*, 9, 35–53. <https://doi.org/10.1016/j.uclim.2014.05.005>
- Bui, D. K., Nguyen, T. N., Ngo, T. D., & Nguyen-Xuan, H. (2020). An artificial neural network (ANN) expert system enhanced with the electromagnetism-based firefly algorithm (EFA) for predicting the energy consumption in building. 190. Energy, Article 116370. <https://doi.org/10.1016/j.energy.2019.116370>
- Chen, H. C., Han, Q., & De Vries, B. (2020). Modeling the spatial relation between urban morphology, land surface temperature and urban energy demand. *Sustainable Cities and Society*, 60, Article 102246. <https://doi.org/10.1016/j.scs.2020.102246>
- Dandotiya, B., & Sharma, H. K. (2021). Climate Change and Its Impact on Terrestrial Ecosystems. In A. Karmaoui, K. Barrick, M. Reed, & M. Baig (Eds.), *Impacts of Climate Change on Agriculture and Aquaculture* (pp. 140–157). IGI Global. <https://doi.org/10.4018/978-1-7998-3343-7.ch007>
- Dogan, T., & Reinhart, C. (2017). Shoeboxer: An algorithm for abstracted rapid multi-zone urban building energy model generation and simulation. *Energy and Buildings*, 140, 140–153. <https://doi.org/10.1016/j.enbuild.2017.01.030>
- Hadavi, M., & Pasdarshahri, H. (2020). Quantifying impacts of wind speed and urban neighborhood layout on the infiltration rate of residential buildings. *Sustainable Cities and Society*, 53, Article 101887. <https://doi.org/10.1016/j.scs.2019.101887>
- Hadavi, M., & Pasdarshahri, H. (2021). Investigating effects of urban configuration and density on urban climate and building systems energy consumption. *Journal of Building Engineering*, 44, Article 102710. <https://doi.org/10.1016/j.jobe.2021.102710>
- Huang, K. T., & Li, Y. J. (2017). Impact of street canyon typology on building's peak cooling energy demand: A parametric analysis using orthogonal experiment. *Energy and Buildings*, 154, 448–464. <https://doi.org/10.1016/j.enbuild.2017.08.054>
- Javanroodi, K., & Nik, V. M. (2019). Impacts of microclimate conditions on the energy performance of buildings in urban areas. *Buildings*, 9(8), 189. <https://doi.org/10.3390/buildings9080189>
- Leng, H., Chen, X., Ma, Y., Wong, N. H., & Ming, T. (2020). Urban morphology and building heating energy consumption: Evidence from Harbin, a severe cold region city. *Energy and Buildings*, 224, Article 110143. <https://doi.org/10.1016/j.enbuild.2020.110143>
- Li, K., Xu, X., Zhang, R., Kong, L., Wang, W., & Deng, W. (2023). Impact of urban form on building energy consumption and solar energy potential: A case study of residential blocks in Jianhu, China. *Energy and Buildings*, 280, Article 112727. <https://doi.org/10.1016/j.enbuild.2022.112727>
- Lu, Y., Chen, Q., Yu, M., Wu, Z., Huang, C., Fu, J., ... Yao, J. (2023). Exploring spatial and environmental heterogeneity affecting energy consumption in commercial buildings using machine learning. *Sustainable Cities and Society*, 95, Article 104586. <https://doi.org/10.1016/j.scs.2023.104586>
- Ma, R., Wang, T., Wang, Y., & Chen, J. (2022). Tuning urban microclimate: A morpho-patch approach for multi-scale building group energy simulation. *Sustainable Cities and Society*, 76, Article 103516. <https://doi.org/10.1016/j.scs.2021.103516>
- Memon, R. A., Leung, D. Y., & Liu, C. H. (2010). Effects of building aspect ratio and wind speed on air temperatures in urban-like street canyons. *Building and Environment*, 45 (1), 176–188. <https://doi.org/10.1016/j.buildenv.2009.05.015>
- Mirkovic, M., & Alawadi, K. (2017). The effect of urban density on energy consumption and solar gains: The study of Abu Dhabi's neighborhood. *Energy Procedia*, 143, 277–282. <https://doi.org/10.1016/j.egypro.2017.12.684>
- Olu-Ajayi, R., Alaka, H., Sulaimon, I., Sunmola, F., & Ajayi, S. (2022). Building energy consumption prediction for residential buildings using deep learning and other machine learning techniques. *Journal of Building Engineering*, 45, Article 103406. <https://doi.org/10.1016/j.jobe.2021.103406>
- Peng, W., Yuan, X., Gao, W., Wang, R., & Chen, W. (2021). Assessment of urban cooling effect based on downscaled land surface temperature: A case study for Fukuoka, Japan. *Urban Climate*, 36, Article 100790. <https://doi.org/10.1016/j.ulclim.2021.100790>
- Quan, S. J., & Li, C. (2021). Urban form and building energy use: A systematic review of measures, mechanisms, and methodologies. *Renewable and Sustainable Energy Reviews*, 139, Article 110662. <https://doi.org/10.1016/j.rser.2020.110662>
- Rickwood, P., Glazebrook, G., & Searle, G. (2008). Urban structure and energy—a review. *Urban policy and research*, 26(1), 57–81. <https://doi.org/10.1080/08111140701629886>
- Santamouris, M. (2020). Recent progress on urban overheating and heat island research. Integrated assessment of the energy, environmental, vulnerability and health impact. Synergies with the global climate change. *Energy and Buildings*, 207, Article 109482. <https://doi.org/10.1016/j.enbuild.2019.109482>
- Seyedzadeh, S., Rahimian, F. P., Rastogi, P., & Glesk, I. (2019). Tuning machine learning models for prediction of building energy loads. *Sustainable Cities and Society*, 47, Article 101484. <https://doi.org/10.1016/j.scs.2019.101484>
- Shan, X., Deng, Q., Tang, Z., Wu, Z., & Wang, W. (2022). An integrated data mining-based approach to identify key building and urban features of different energy usage levels. *Sustainable Cities and Society*, 77, Article 103576. <https://doi.org/10.1016/j.scs.2021.103576>
- Shareef, S. (2021). The impact of urban morphology and building's height diversity on energy consumption at urban scale: The case study of Dubai. *Building and Environment*, 194, Article 107675. <https://doi.org/10.1016/j.buildenv.2021.107675>
- Sharifi, A. (2019). Resilient urban forms: A review of literature on streets and street networks. *Building and Environment*, 147, 171–187. <https://doi.org/10.1016/j.buildenv.2018.09.040>
- Somu, N., MR, G. R., & Ramamirtham, K. (2021). A deep learning framework for building energy consumption forecast. *Renewable and Sustainable Energy Reviews*, 137, Article 110591. <https://doi.org/10.1016/j.rser.2020.110591>
- Street, M., Reinhart, C., Norford, L., & Ochsendorf, J. (2013). Urban heat island in Boston—an evaluation of urban air temperature models for predicting building energy use. *Building Simulation*, 1022–1029.
- Strømann-Andersen, J., & Satrapp, P. A. (2011). The urban canyon and building energy use: Urban density versus daylight and passive solar gains. *Energy and Buildings*, 43 (8), 2011–2020. <https://doi.org/10.1016/j.enbuild.2011.04.007>
- Tehrani, A. A., Veisi, O., Fakhr, B. V., & Du, D. (2024). Predicting solar radiation in the urban area: A data-driven analysis for sustainable city planning using artificial neural networking. *Sustainable Cities and Society*, 100, Article 105042. <https://doi.org/10.1016/j.scs.2023.105042>
- Uçlar, S., & Bulduruk, M. A. (2020). Relation between urban form and heating energy consumption. A/Z ITU Journal of Faculty of Architecture, 17(3), 89–101. <https://doi.org/10.5505/itufja.2020.09787>
- Wang, M., Yu, H., Yang, Y., Jing, R., Tang, Y., & Li, C. (2022). Assessing the impacts of urban morphology factors on the energy performance for building stocks based on a novel automatic generation framework. *Sustainable Cities and Society*, 87, Article 104267. <https://doi.org/10.1016/j.scs.2022.104267>
- Wang, P., Liu, Z., & Zhang, L. (2021). Sustainability of compact cities: A review of Inter-Building Effect on building energy and solar energy use. *Sustainable Cities and Society*, 72, Article 103035. <https://doi.org/10.1016/j.scs.2021.103035>
- Wong, N. H., Jusuf, S. K., Syafii, N. I., Chen, Y., Hajadi, N., Sathyaranayanan, H., & Manickavasagam, Y. V. (2011). Evaluation of the impact of the surrounding urban morphology on building energy consumption. *Solar energy*, 85(1), 57–71. <https://doi.org/10.1016/j.solener.2010.11.002>
- Xi, C., Ren, C., Wang, J., Feng, Z., & Cao, S. J. (2021). Impacts of urban-scale building height diversity on urban climates: A case study of Nanjing, China. *Energy and Buildings*, 251, Article 111350. <https://doi.org/10.1016/j.enbuild.2021.111350>
- Xie, M., Wang, M., Zhong, H., Li, X., Li, B., Mendis, T., & Xu, S. (2023). The impact of urban morphology on the building energy consumption and solar energy generation potential of university dormitory blocks. *Sustainable Cities and Society*, 96, Article 104644. <https://doi.org/10.1016/j.scs.2023.104644>
- Xu, D., Wang, Y., Zhou, D., Wang, Y., Zhang, Q., & Yang, Y. (2024). Influences of urban spatial factors on surface urban heat island effect and its spatial heterogeneity: A case study of Xi'an. *Building and Environment*, 248, Article 111072. <https://doi.org/10.1016/j.buildenv.2023.111072>
- Xu, S., Jiang, H., Xiong, F., Zhang, C., Xie, M., & Li, Z. (2021). Evaluation for block-scale solar energy potential of industrial block and optimization of application strategies: A case study of Wuhan, China. *Sustainable Cities and Society*, 72, Article 103000. <https://doi.org/10.1016/j.scs.2021.103000>
- Xu, S., Sang, M., Xie, M., Xiong, F., Mendis, T., & Xiang, X. (2023). Influence of urban morphological factors on building energy consumption combined with photovoltaic potential: A case study of residential blocks in central China. *Building Simulation*, 16 (9), 1777–1792. <https://doi.org/10.1007/s12273-023-1014-4>
- Yang, X., Peng, L. L., Jiang, Z., Chen, Y., Yao, L., He, Y., & Xu, T. (2020). Impact of urban heat island on energy demand in buildings: Local climate zones in Nanjing. *Applied Energy*, 260, Article 114279. <https://doi.org/10.1016/j.apenergy.2019.114279>
- Yang, Y., Chen, Y., Wang, Y., Li, C., & Li, L. (2016). Modelling a combined method based on ANFIS and neural network improved by DE algorithm: A case study for short-term electricity demand forecasting. *Applied Soft Computing*, 49, 663–675. <https://doi.org/10.1016/j.asoc.2016.07.053>
- Yue, Y., Yan, Z., Ni, P., Lei, F., & Qin, G. (2024). Promoting solar energy utilization: Prediction, analysis and evaluation of solar radiation on building surfaces at city scale. *Energy and Buildings*, 319, 114561. <https://doi.org/10.1016/j.enbuild.2024.114561>
- Zhang, J., Cui, P., & Song, H. (2020). Impact of urban morphology on outdoor air temperature and microclimate optimization strategy base on Pareto optimality in Northeast China. *Building and Environment*, 180, Article 107035. <https://doi.org/10.1016/j.buildenv.2020.107035>

Zhang, M., & Gao, Z. (2021). Effect of urban form on microclimate and energy loads: Case study of generic residential district prototypes in Nanjing, China. *Sustainable Cities and Society*, 70, Article 102930. <https://doi.org/10.1016/j.scs.2021.102930>

Zhang, X., Yan, F., Liu, H., & Qiao, Z. (2021). Towards low carbon cities: A machine learning method for predicting urban blocks carbon emissions (UBCE) based on built

environment factors (BEF) in Changxing City, China. *Sustainable Cities and Society*, 69, Article 102875. <https://doi.org/10.1016/j.scs.2021.102875>

Zhao, Y., Ding, X., Wu, Z., Yin, S., Fan, Y., & Ge, J. (2024). Impact of urban form on building energy consumption in different climate zones of China. *Energy and Buildings*, 320, 114579. <https://doi.org/10.1016/j.enbuild.2024.114579>